https://doi.org/10.5194/egusphere-2023-1826
Preprint. Discussion started: 5 September 2023

An effective machine learning approach for predicting ecosystem CO_2 assimilation across space and time

Piersilvio De Bartolomeis[1,⋆], Alexandru Meterez[1,⋆], Zixin Shu[1,⋆,*], Benjamin D. Stocker[2,3,4]

[1] Department of Computer Science, ETH Zürich
[2] Department for Environmental System Science, ETH Zürich
[3] Institute of Geography, University of Bern, Hallerstrasse 12, 3012 Bern, Switzerland
[4] Oeschger Centre for Climate Change Research, University of Bern, Falkenplatz 16, 3012 Bern, Switzerland
⋆ These authors contributed equally to this work.

Correspondence: piersilvio.debartolomeis@inf.ethz.ch

Abstract. Accurate predictions of environmental controls on ecosystem photosynthesis are essential for understanding the impacts of climate change and extreme events on the carbon cycle and the provisioning of ecosystem services. Using time-series measurements of ecosystem fluxes paired with measurements of meteorological variables from a network of globally distributed sites and remotely sensed vegetation indices, we train a recurrent deep neural network (Long-Short-Term Memory, LSTM), a simple deep neural network (DNN), and a mechanistic, theory-based photosynthesis model with the aim to predict ecosystem gross primary production (GPP). We test these models' ability to spatially and temporally generalise across a wide range of environmental conditions. Both neural network models outperform the theory-based model considering leave-site-out cross-validation (LSOCV). The LSTM model performs best and achieves a mean R^2 of 0.78 across sites in the LSOCV and an average R^2 of 0.82 across relatively moist temperate and boreal sites. This suggests that recurrent deep neural networks provide a basis for robust data-driven ecosystem photosynthesis modelling in respective biomes. However, limits to global model upscaling are identified using cross-validation by vegetation types and by continents. In particular, our model performance is weakest at relatively arid sites where unknown vegetation exposure to water limitation limits model reliability.

1 Introduction

CO_2 assimilation by photosynthesis is the "engine" of the carbon cycle and provides energy for ecosystem processes. Understanding its controls and variations across time and space is key for accurate predictions of climate impacts on the terrestrial biosphere and Earth system feedbacks. Gross primary production (GPP), the ecosystem-level photosynthetic CO_2 assimilation, varies across different scales, reflecting variations in the environment across Earth's biomes (Wang et al., 2014), across diurnal and seasonal cycles, between years (Ahlström et al., 2015), and in response to climate extremes (Ciais et al., 2005) and their legacies at longer time scales (days to years) (Bastos et al., 2020).

GPP variations are driven by multiple, simultaneously varying environmental factors and the physiological and structural responses of plants. Solar radiation supplies the energy for photosynthesis. Together with the canopy structure, determining

*currently affiliated with the ARTORG Center for Biomedical Engineering Research, University of Bern

https://doi.org/10.5194/egusphere-2023-1826
Preprint. Discussion started: 5 September 2023

light absorption, it acts as a dominant driver of GPP (Monteith, 1972). Temperature, light, and water availability trigger phenological changes and govern seasonal cycles of active leaf surface area and are thus underlying seasonal changes in light absorption. Air temperature affects leaf temperatures, which in turn govern enzymatic rates and photosynthesis. Low moisture availability across the rooting zone, in combination with a high vapour pressure deficit of air at the leaf surface, determines the effects of water stress and can lead to GPP reductions (Stocker et al., 2018a; Novick et al., 2016). GPP is also affected by gradual physiological changes evolving over daily to seasonal time scales (Jiang et al., 2020), long-term effects of past stress (Bastos et al., 2020; Yu et al., 2022), and the amount of active foliage area deployed to intercept solar radiation and harvest its energy. Physiological changes are caused, e.g., by the seasonal acclimation of the photosynthetic apparatus to varying levels of radiation inputs and temperature (Kumarathunge et al., 2019a; Luo and Keenan, 2020a; Jiang et al., 2020).

Continuous GPP estimates can be obtained from eddy covariance measurements of ecosystem gas exchange (Baldocchi, 2020) and capture surface-atmosphere exchange fluxes, integrated over a radius on the order of a kilometre around the site of measurement (Chu et al., 2021). A large volume of such data, standardised, and measured in parallel with a comprehensive set of meteorological variables and soil conditions (temperature and moisture), are made available through different networks and initiatives (e.g., Ameriflux, ICOS, OzFlux). The FLUXNET2015 dataset was created using standardized processing of eddy covariance measurements of a large number of sites from multiple regional networks and has been made openly accessible in a standardized format (Pastorello et al., 2020a). Its large data volume gives rise to opportunities for data-driven machine learning methods for predicting spatiotemporal variations of ecosystem-atmosphere exchange fluxes, modelled on the basis of environmental covariates (Jung et al., 2020, 2011). Thanks to the combination of temporally resolved data, available from a large number of sites, covering a wide envelope of environmental conditions, spatial generalisation can be attempted. That is, predictive methods may be developed to model ecosystem fluxes at geographical locations from which no data was used during model training. Such spatially upscaled estimates are valuable for estimating temporal variations of C and water fluxes across larger areas and carbon cycle impacts by climate extremes (Jung et al., 2010). Spatio-temporally upscaled, data-driven estimates are widely used for estimating fluxes of the global carbon cycle and for benchmarking mechanistic models (Wiltshire et al., 2020; Peng et al., 2015; Sun et al., 2018).

However, concerns have been raised about the reliability of spatial upscaling using data-driven models that are trained on ecological data that is typically representative of a limited geographical and environmental space (Ploton et al., 2020; Meyer and Pebesma, 2022). Parameter-rich, but "data-hungry" machine learning models appear to be successful at predicting ecological quantities when trained and tested against the limited available data. However, their flexibility and risk of overfitting may come at the expense of poor model generalisability to conditions that are poorly or not at all represented in the training data.

GPP can be conceived as a function of a set of environmental covariates, whereby models are formulated assuming independent and identically distributed (IID) observations. However, this assumption is violated by the non-stationarity of relationships between GPP and the environment. Such non-stationarities arise from multiple processes. e.g., plant hydraulic processes induce a temporal hysteresis effect over the course of diurnal cycles (Tuzet et al., 2003). Seasonally varying physiological and phenological changes alter relationships between GPP and the abiotic environment (Kumarathunge et al., 2019a; Luo and Keenan, 2020a). Stress by extreme environmental conditions in the past can cause long-lasting effects, caused by impaired

https://doi.org/10.5194/egusphere-2023-1826
Preprint. Discussion started: 5 September 2023

transpiration and reduced assimilation (Barber and Andersson, 1992; McDowell et al., 2022). Some of these limitations to modelling GPP under the IID assumption may be relieved by temporal aggregation of modelled data to daily-monthly time scales and by pairing data with additional, remotely sensed observations that capture phenological changes and variations in the amount of active, light-intercepting foliage area (Baldocchi, 2018). Satellite data products of the surface reflectance are widely used for providing information about spatially and seasonally varying vegetation structure and light absorption (Ryu et al., 2019). However, additional physiological changes that affect the efficiency of light utilization for CO_2 assimilation at the leaf level are more challenging to capture by remotely sensed reflectance data (Gamon et al., 2016). As a consequence, substantial unexplained GPP variation is expected to remain, in particular at the seasonal time scale.

Published machine-learning (ML) based GPP models used for spatiotemporal modelling typically rely on the IID assumption (Yang et al., 2007; Beer et al., 2010; Xiao et al., 2010; Jung et al., 2011, 2020; Tramontana et al., 2016) and thus lack the capacity to learn temporal dependencies. This limitation may be relieved by "time-aware" ML algorithms that learn non-stationary relationships and temporal dependencies. Recurrent neural networks with Long Short-Term Memory (LSTM) cells have been shown to be highly successful at tasks where memory effects across a range of temporal scales are involved (Hochreiter and Schmidhuber, 1997). Today, such models underlie most solutions for language-related tasks and time series modelling (D. and L., 2013; Elsworth and Güttel, 2020).

The aim of this paper is twofold and addresses the following two research questions:

- Are machine-learning models that learn temporal structure in the data suitable for predicting GPP? To address this question, we evaluate the performance of an LSTM model on unseen test sites (leave-site-out cross-validation) and compare it with the results of a non-recurrent DNN that relies on the IID assumption, and with a theory-based GPP model, the P-model (Stocker et al., 2015; Wang et al., 2017; Prentice et al., 2014) that models the acclimation of leaf physiology and relies on a very small number of model parameters.

- How well can we up-scale fluxes for mapping GPP time series for temporal flux time series mapping? To address this question, we assess the generalisability of the LSTM-based GPP model in geographic and environmental space, and in terms of generalisations to new vegetation types.

2 Methods

2.1 The prediction challenge

The general structure of a model f for spatial generalisations of time series data can be described as

$$y_{i,t+N} = f(\mathbf{x}_{i,t+(M..N)}, \mathbf{z}_i) \,, \tag{1}$$

where y is the target variable (here GPP), $\mathbf{x}$ is a vector of temporally resolved covariates (predictors), $\mathbf{z}$ is a vector of time-invariant information (e.g., vegetation type), index i refers to a location in geographical space, and t is the time step. As formulated here, the prediction of y for a future time step $t+N$ depends on the history of environmental covariates ($t+(M..N)$).

https://doi.org/10.5194/egusphere-2023-1826
Preprint. Discussion started: 5 September 2023

Models using the IID assumption neglect this history and can be described as $y_{i,t} = f(\mathbf{x}_{i,t}, \mathbf{z}_i)$. Note that in both cases, no spatial context $\mathbf{x}_j$ or $\mathbf{z}_j$ $(i \neq j)$, nor explicit information about the geographical location $(y_i = f(i, ...))$ is used for modelling y_i.

2.2 Data selection

For training and testing the model, we use FLUXNET2015 data at the daily resolution (Pastorello et al., 2020b). We used GPP based on the night-time flux partitioning (Reichstein et al., 2005), and the variable u^*-threshold method (GPP_NT_VUT_REF in the dataset). The daily FLUXNET2015 data is based on sums of half-hourly data. We used only data from days where more than 80% of the underlying half-hourly data was good-quality, measured data (not gap-filled). We used the following temporally resolved metereological covariates, measured in parallel at eddy covariance sites and provided as part of the FLUXNET2015 dataset as daily means, unless specified otherwise (variable name given in brackets): air temperature (TA_F), daytime mean air temperature (TA_F_DAY), nighttime mean air temperature (TA_F_NIGHT), shortwave incoming radiation (SW_IN_F), long-wave incoming radiation (LW_IN_F), vapour pressure deficit (VPD_F), atmospheric pressure (PA_F), daily total precipitation (P_F), and wind speed (WS_F). Soil water content data was unavailable for many sites and missing particularly for deep soil layers. For this reason, we used soil moisture modelled using a simple water balance model, forced with observed precipitation and modelled evapotranspiration (Davis et al., 2017; Stocker et al., 2015).

To complement site-level measurements, we used remotely sensed estimates for the fraction of absorbed photosynthetically active radiation (fAPAR), extracted from the MODIS FPAR MCD15A3H collection 6 product (Myneni et al., 2015). fAPAR captures variations in phenology and the amount of solar radiation absorbed by the canopy and usable for photosynthesis. fAPAR data is extracted for the center pixel (500 m lateral extent), surrounding each measurement site. fAPAR data cleaning was implemented to keep only good quality data (i.e., derived using the main data retrieval algorithm) and data that are not affected by significant clouds. fAPAR data are provided at a 4-day resolution and were interpolated to a daily time step using a LOESS spline. All fAPAR data download and processing is implemented using the *ingestr* and *MODISTools* R packages (Stocker and Hufkens, 2021; Tuck et al., 2014). As time-invariant information, we used information about the dominant vegetation type at respective sites (see Table 1), obtained through the FLUXNET2015 dataset.

We selected data from 53 sites (Fig. 1, Tab. 1) where data from at least 500 days was available, and where a previous analysis yielded robust (site-specific) relationships between GPP and a similar set of environental covariates (Stocker et al., 2018b).

2.3 Data pre-processing

All pre-processing steps (imputation and standardization) were done for each site separately. This avoids data leakage, arising from applying data transformation with parameters derived from the testing portion of the data. We imputed missing GPP values (16.5%) using K-Nearest Neighbors (KNN) imputation with all available environmental covariates (see above). Time series of daytime and nighttime mean air temperature had a very small portion of missing values (0.002%) and were also filled with KNN imputation, using daily mean temperature and shortwave incoming radiation as predictors. We also had to drop

https://doi.org/10.5194/egusphere-2023-1826
Preprint. Discussion started: 5 September 2023

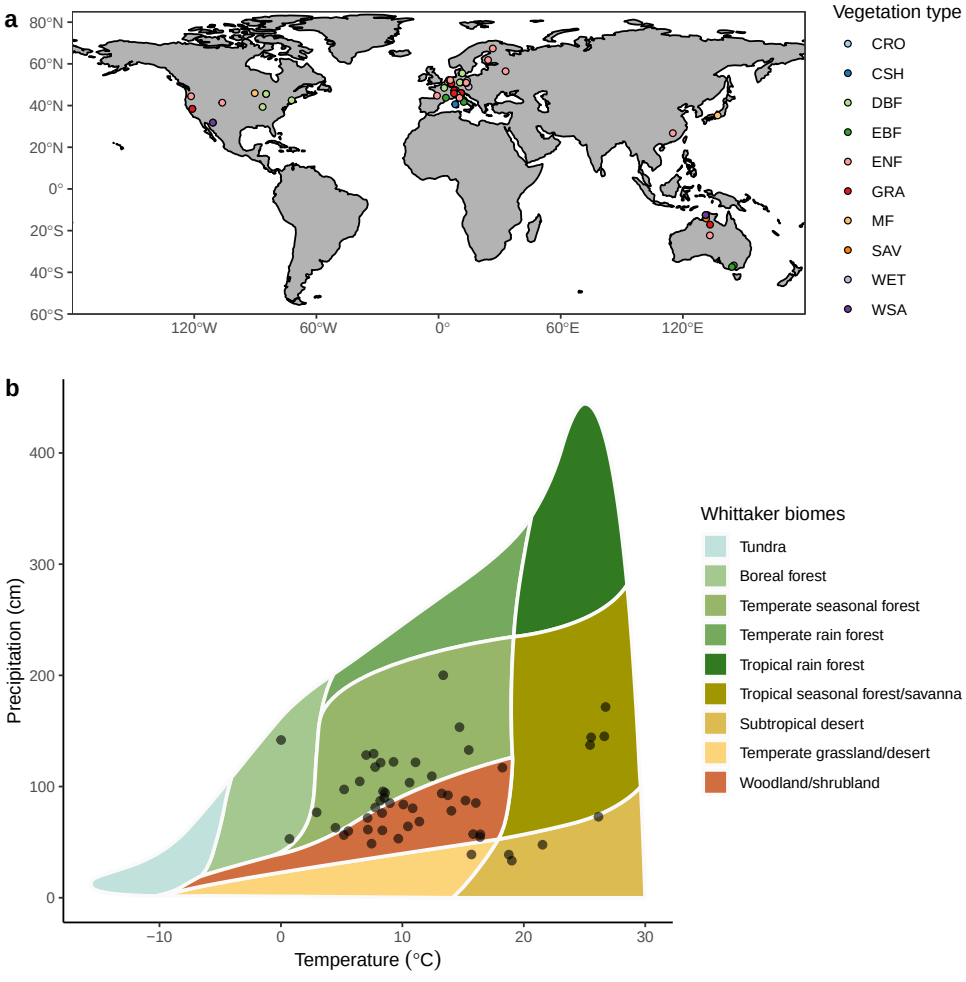

Figure 1. Locations of selected sites in geographical space (a) and environmental space (b). Colors of points in (a) indicate the predominant vegetation type present at respective sites (GRA: grasslands, SAV: savannah, WSA: woody savannah, ENF: evergreen needleleaved forest, EBF: evergreen broadleaved forest, DBF: deciduous broadleaved forest, CSH: closed shrubland, WET: wetland, CRO: cropland, MF: mixed forest). In (b), axes indicate the environmental space and are defined by the mean annual precipitation and temperature and colors delineate biomes defined by (Whittaker, 1962), plotted using the *plotbiomes* R library (Stefan and Levin, 2023).

https://doi.org/10.5194/egusphere-2023-1826
Preprint. Discussion started: 5 September 2023

the site "CN-Cng" because meta-data information was missing. The categorical time-invariant predictor (vegetation type) was one-hot encoded.

2.4 Model architectures

We evaluated two different machine learning algorithms to compare the suitability of different model architectures for the spatiotemporal prediction task at hand. To account for temporal dependencies in the data, we used a deep neural network with a Long Short-Term Memory (LSTM) cell implemented in PyTorch. LSTMs belong to the class of recurrent neural networks. Applying such a model architecture to the present prediction task enables the modelling of GPP in an autoregressive manner (see Equation 1). The architecture implemented here consists of a single LSTM cell, combined with a multilayer perceptron (MLP, Fig. 2). The MLP architecture consisted of four linear, fully-connected layers with 11, 64, 32 and 16 nodes, respectively. For each timestep, the output of the LSTM is passed through an MLP to obtain the final value. The combination of the LSTM and MLP is chosen to introduce additional nonlinearity in the LSTM output and reduce the bias of the output sequence. The weights of the MLPs are shared between all timesteps.

In addition to the LSTM, we trained a deep neural network (henceforth referred to as 'DNN') as an MLP using PyTorch (Paszke et al., 2019). The model architecture consisted of four linear, fully-connected layers with 11, 64, 32 and 16 nodes, respectively. ReLu functions were used as the activation function between each layer. We trained the DNN model using an Adam optimizer with a learning rate of 3×10^{-4} and a batch size of one and considered the mean squared error as the loss function.

The theory-based photosynthesis model is the P-model (Prentice et al., 2014; Wang et al., 2017; Stocker et al., 2020). The P-model combines established theory for C3 photosynthesis following the Farquhar-von Caemmerer-Berry (FvCB) model with the least cost hypothesis for the optimal balancing of water loss and carbon gain (Prentice et al., 2014), and the coordination hypothesis (Maire et al., 2012; Wang et al., 2017) which states that the light and Rubisco-limited assimilation rates (as described by the FvCB model) are equal for representative daytime environmental conditions. Based on these theoretical foundations, GPP can be modelled as the product of absorbed photosynthetically active radiation, specified by the locally measured photosynthetically active radiation (PAR) and remotely sensed fAPAR, and the theory-based prediction of the ecosystem-level light use efficiency, as described in more detail by (Stocker et al., 2020). For the analyses presented here, we used model outputs of the leave-site-out cross-validation presented in(Stocker et al., 2020) (referred to as 'out-of-sample evaluation' therein) with the model setup that included a soil moisture stress function and a temperature-dependent quantum yield (which acts as a linear scalar on ecosystem light use efficiency), corresponding to the simulation setup 'FULL' in (Stocker et al., 2020). For these simulations, three model parameters for calibrated to GPP data from FLUXNET: one parameter specifying the apparent ecosystem-level quantum yield and two parameters specifying the soil moisture stress function and how it varies with mean site aridity. The calibration was implemented as a parameter optimization, minimising the root mean square error, using the generalised simulated annealing algorithm implemented by the *GenSA* R package (Yang Xiang et al., 2013).

https://doi.org/10.5194/egusphere-2023-1826
Preprint. Discussion started: 5 September 2023

2.5 LSTM and DNN model training

We trained the models using an Adam optimizer with a learning rate of 3×10^{-4} and considered the mean squared error as the loss function. Because the sequences (number of data points per site) had very different lengths, we used a batch size of one to avoid zero-padding or decimating the long sequences. To reduce the model overfitting, we used *dropout* as a regularizer with probability 0. The models were implemented using PyTorch (Paszke et al., 2019).

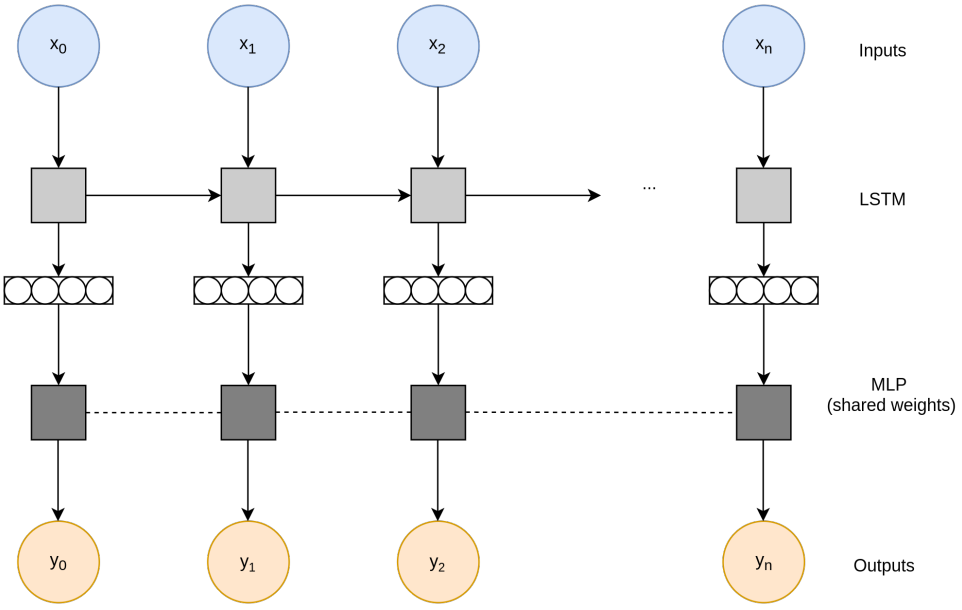

Figure 2. Architecture of the LSTM model. Inputs $x_{0..n}$ are vectors of predictors at each time step and are used as inputs to the LSTM cell. The output of the LSTM cell is a vector (illustrated by multiple, boxed circles) and used as input to the MLP, which uses shared weights across time steps. The outputs $y_{0..n}$ receive the value from the output node of the MLP and constitute the model prediction of the target variable - here GPP.

2.6 Model evaluation

Model evaluation was based on leave-site-out-cross-validation (LSOCV) and leave-group-out-cross-validation (LGOCV). In LSOCV, we trained on all but one site and tested predictions for the remaining site. In LGOCV, we trained on all but one group and tested predictions on the remaining group. The groups we used for testing were vegetation types and continents (sites in the US and outside the US). LGOCV, where sites are grouped by vegetation types, assesses the generalization performance for out-of-sample vegetation types. Poor performance, for LGOCV determined as the model bias, indicates that relationships between y and $\mathbf{x}$ are substantially modulated by vegetation type-specific properties, e.g., due to differences in canopy radiation transfer and absorption between broadleaved and coniferous forests. LGOCV, where sites are grouped by continents, assesses

https://doi.org/10.5194/egusphere-2023-1826
Preprint. Discussion started: 5 September 2023

the generalization performance of spatial upscaling across large geographic scales, and potentially to ecosystems with different floral compositions on different continents.

For the LSOCV, we computed evaluation metrics (coefficient of determination, R^2; root mean squared error, RMSE) on predictions for the left-out site, pooled from all sites, and as the mean across evaluation metrics determined on predictions for sites separately. For the LGOCV, we quantified the bias (difference between predicted and observed GPP) and the RMSE.

In addition to deriving performance metrics from the LSOCV based on daily data, we aggregated predictions and observations to different scales (mean seasonal cycle, annual, site-level) and pooled predicted and observed values from all sites before calculating performance metrics. This measures complimentary aspects of model performance and enables comparability to other studies. The mean seasonal cycle was determined as the mean by day-of-year for each site separately. Daily anomalies were derived as the difference of daily values to the site-specific mean seasonal cycle. Additionally, we evaluated the mean seasonal cycle per climate zone, where sites were grouped based on a global map of Koeppen-Geiger climate classes (Beck et al., 2018). Annual anomalies were determined as the annual values by site minus the mean across years by site.

To interpret the link between out-of-sample prediction skill and site characteristics, we investigated the relationships of site-specific R^2 of modelled versus observed GPP from the LSOCV with a set of variables that characterise the site conditions (moisture index, vegetation type, climate zone). The moisture index was defined as the ratio of mean annual precipitation over potential evapotranspiration (PET), derived from locally measured precipitation and PET estimated based on Priestly-Taylor (Priestley and Taylor, 1972) as implemented in the SPLASH ecosystem water balance model (Davis et al., 2017). The site's dominant vegetation type was identified based on meta-information provided through FLUXNET2015 (Pastorello et al., 2020a). The site's climate zone was identified based on the Koeppen-Geiger classification with information extracted from a global map by (Beck et al., 2018).

3 Results

3.1 Leave-site-out cross-validation

The LSTM outperforms other models in predicting GPP. For daily values, the mean R^2, determined as a mean across sites from the LSOCV, is 0.78 for the LSTM, 0.73 for the DNN, and 0.64 for the P-model (Tab. 3). Model performances vary substantially across sites (Fig. 3) and the weakest model performance is evident for the same sites for all models. The improvement of model performance of the LSTM over the P-model is evident for almost all sites, except a few (mostly dry) sites. We also compared the performance of the "standard" LSTM against an LSTM model trained with both time-invariant and time-dependent variables but did not find any significant improvement when adding the time-invariant features to the learning problem (not shown).

3.2 Model performance across scales

The LSTM outperforms other models across all scales (Tab. 3). The somewhat higher R^2 derived for pooled daily values, compared to the LSOCV-mean, reflects the fact that relatively poor model performance tends to be found at sites for which

https://doi.org/10.5194/egusphere-2023-1826
Preprint. Discussion started: 5 September 2023

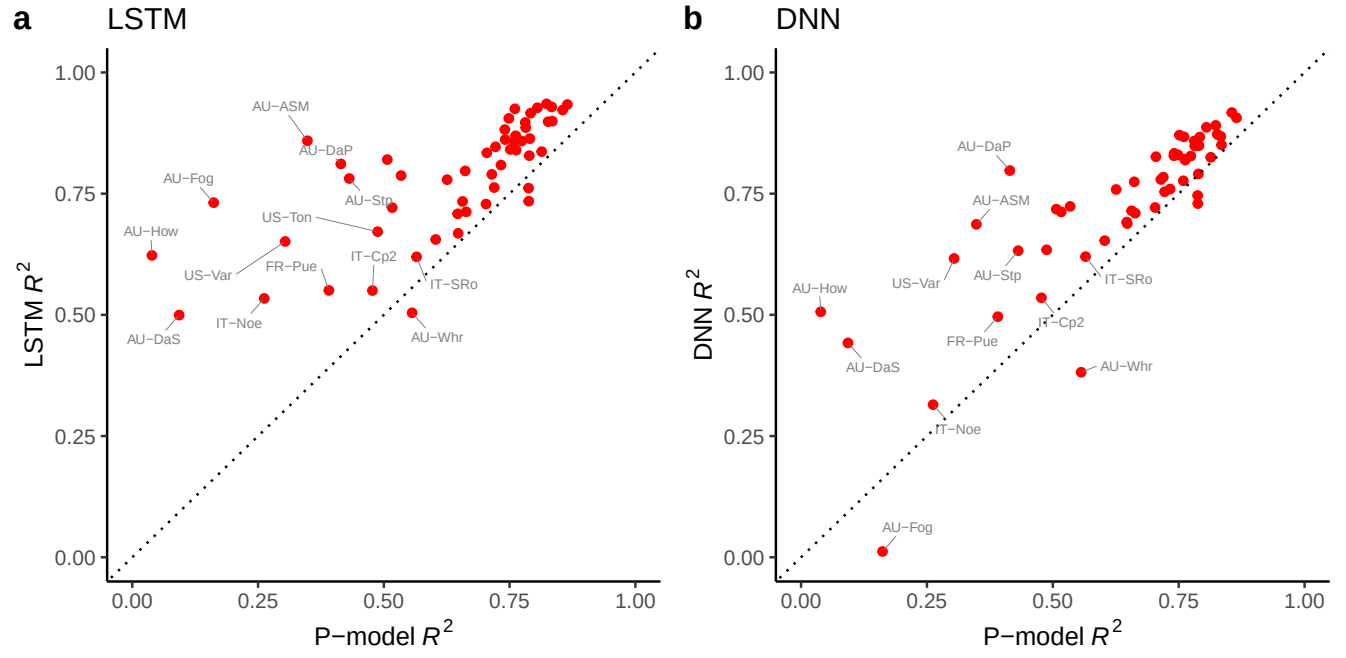

Figure 3. Benchmarking of the LSTM (a) and DNN (b) models against the P-model. R^2 of predicted versus observed daily values from the LSOCV are shown for the LSTM and the DNN models along the y-axis and for the P-model along the x-axis. Points lying above the dotted (1:1) line indicate that the LSTM (DNN) model outperforms the P-model for the respective site. Selected site names are indicated by grey labels.

fewer data is available. The superior performance of the LSTM model over the DNN appears to be linked to its superior performance in capturing seasonal effects, spatial variations, and daily, but not annual anomalies. The good performance of the LSTM on seasonal variations reflects the ability of the LSTM to effectively learn temporal dependencies at weekly to monthly scales. Compared to variations at other scales, seasonal variations are confidently predicted by all models and respective R^2 values are higher compared to values from evaluations on other scales.

A clearer distinction of model performance for simulating the seasonal course of GPP is revealed by the visualisation of modelled and observed mean seasonal cycles by climate zone Fig. 4. The LSTM performs better than the DNN in multiple aspects, including the peak (wet)-season GPP for tropical savannah ('Aw'), and the timing of GPP increases in early spring in sites with a mesic temperate or a boreal climate ('Cfa', and 'Dfb'). The evaluation of GPP on sites located in climates that are marked with a warm and arid summer ('Csa', 'Csb') reveals a substantial bias for both the LSTM and the DNN models. However, also here, the LSTM performs better than the DNN in capturing the seasonal course of GPP.

https://doi.org/10.5194/egusphere-2023-1826
Preprint. Discussion started: 5 September 2023

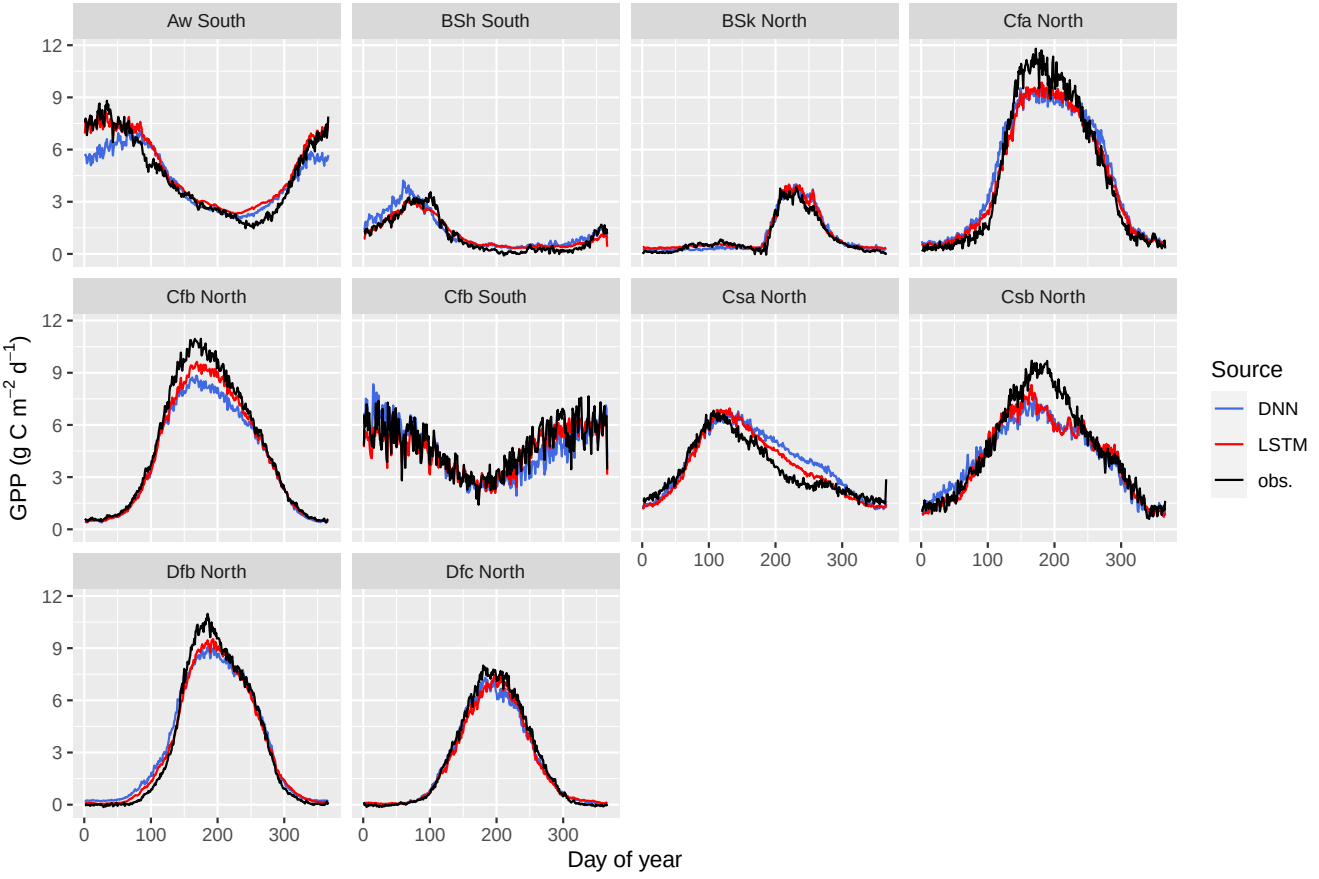

Figure 4. Mean seasonal cycle of GPP by climate zone, separated into zones in the northern and southern hemisphere. Predictions extracted from the LSOCV for DNN and LSTM are compared against observations ('obs.'). Climate zone information is extracted per site from Beck et al. (2018). 'Aw' is tropical savannah, 'Bsh' is arid hot steppe, 'Bsk' is arid cold steppe, 'Cfa' is warm temperate fully humid with hot summer, 'Cfb' is warm temperate fully humid with warm summer, 'Csa' is warm temperate with dry and hot summer, 'Csb' is warm temperate with dry and warm summer, 'Dfb' is cold fully humid with warm summer, 'Dfc' is cold fully humid with cold summer.

3.3 Patterns in out-of-sample prediction skill

Overall, the LSTM yielded the best out-of-sample predictions for relatively moist, temperate or cool sites, and particularly for those with a deciduous vegetation type. For a moisture index of P/PET> 1.25, the average LSOCV-R^2 of predicted versus observed GPP was 0.82. For sites with deciduous broadleaved forest vegetation, the average LSOCV-R^2 was 0.91. The average LSOCV-R^2 was 0.86 for sites with a temperature-controlled, but not water-limited growing season (climate zones 'Cfa', 'Dfc', 'Dfb').

In contrast, we found that all sites with relatively poor out-of-sample prediction skill (LSOCV-$R^2 < 0.7$) were located in relatively dry climates (P/PET < 1.0), except for AU-How and CH-Oe1, where the LSOCV-R^2 was < 0.7 while PET was

https://doi.org/10.5194/egusphere-2023-1826
Preprint. Discussion started: 5 September 2023

>1.0. However, a dry climate was not sufficient to yield poor out-of-sample prediction performance. For several dry sites, the LSTM performed well (e.g., AU-ASM, US-SRM, US-SRG, AU-Stp). There was a clear pattern between out-of-sample prediction skill and vegetation type. The LSTM's out-of-sample prediction skill was relatively poor (LSOCV-$R^2 < 0.6$) for savannah, closed shrubland, and evergreen broadleaved forest sites (except for AU-Wom). All sites for which the LSOCV-R^2 was < 0.7 belonged to either temperate climate zones with a warm and/or dry summer ('Cfb' and 'Csa', the latter being a mediterranean climate) or to a tropical savannah climate ('Aw').

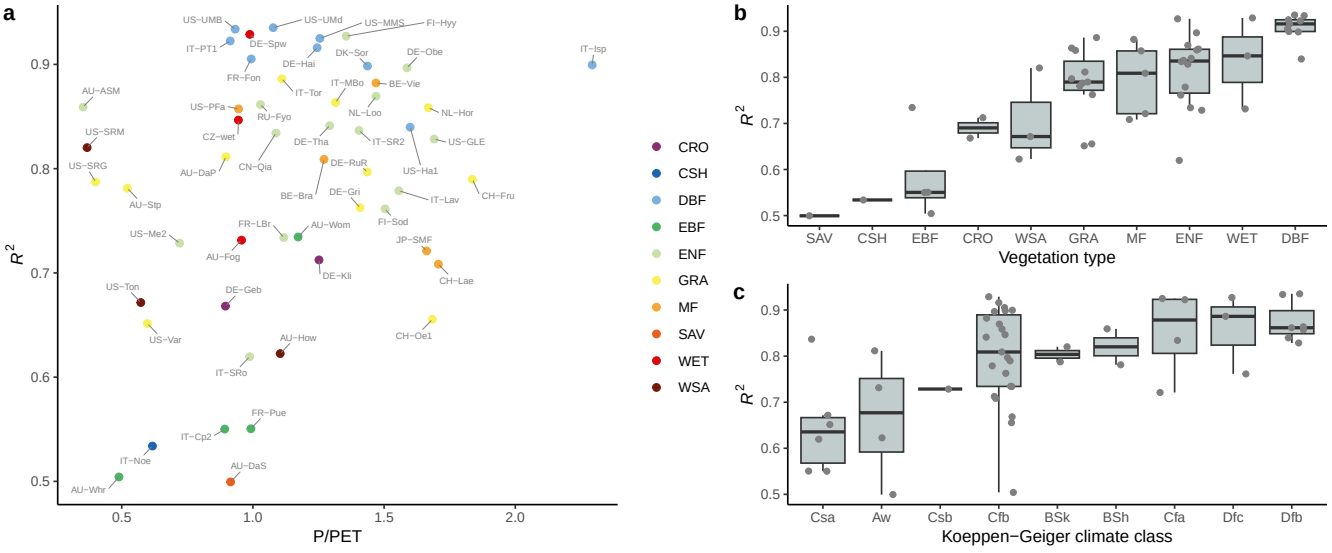

Figure 5. Patterns in out-of-sample prediction skill, measured by the R^2 of modelled vs. observed GPP from the LSTM model, determined from the LSOCV. (a) LSOCV-R^2 versus the moisture index, defined as the ratio of precipitation over potential evapotranspiration (P/PET). The color of points indicates the dominant vegetation type at the respective site. 'CRO' are croplands, 'CSH' are closed shrublands, 'DBF' are deciduous broadleaved forests, 'EBF' are evergreen broadleaved forests, 'ENF' are evergreen needleleaved forests, 'GRA' are grasslands, 'MF' are mixed forests, 'SAV' are savannahs, 'WET' are wetlands, 'WSA' are woody savannahs. (b) LSOCV-R^2 by vegetation types, (c) LSOCV-R^2 by climate zones. See the caption of Fig. 4 for an explanation of abbreviations of climate zones.

3.4 Generalisability across vegetation types

The LGOCV with vegetation types shows that models trained with data from sites of a certain, single vegetation type perform best when predicting GPP on the same vegetation type (Fig. 6). In contrast, predictions made for a vegetation type that was not represented in the training data are poorer. This is most clearly expressed for grassland vs. non-grassland model training and testing (Fig. 6b), where models trained on sites with forest vegetation yield predictions that tend to be positively biased and have a higher RMSE (2.23 - 4.15 gC m^{-2} d^{-1}) when predicting on grassland sites. In contrast, the model trained on grassland data achieves an RMSE of 1.98 gC m^{-2} d^{-1} when predicting on (out-of-sample) grassland sites. However, the model that is trained on data from all vegetation types achieves good performance on all vegetation types - similar to the model that is

https://doi.org/10.5194/egusphere-2023-1826
Preprint. Discussion started: 5 September 2023

trained and tested on the same vegetation type (measured by predictions from the LSOCV). For the case of mixed forests and for grasslands, the model trained on data from all vegetation types yields even better performance than the model trained on data from only MF, or only GRA, respectively (Fig. 6 b and d).

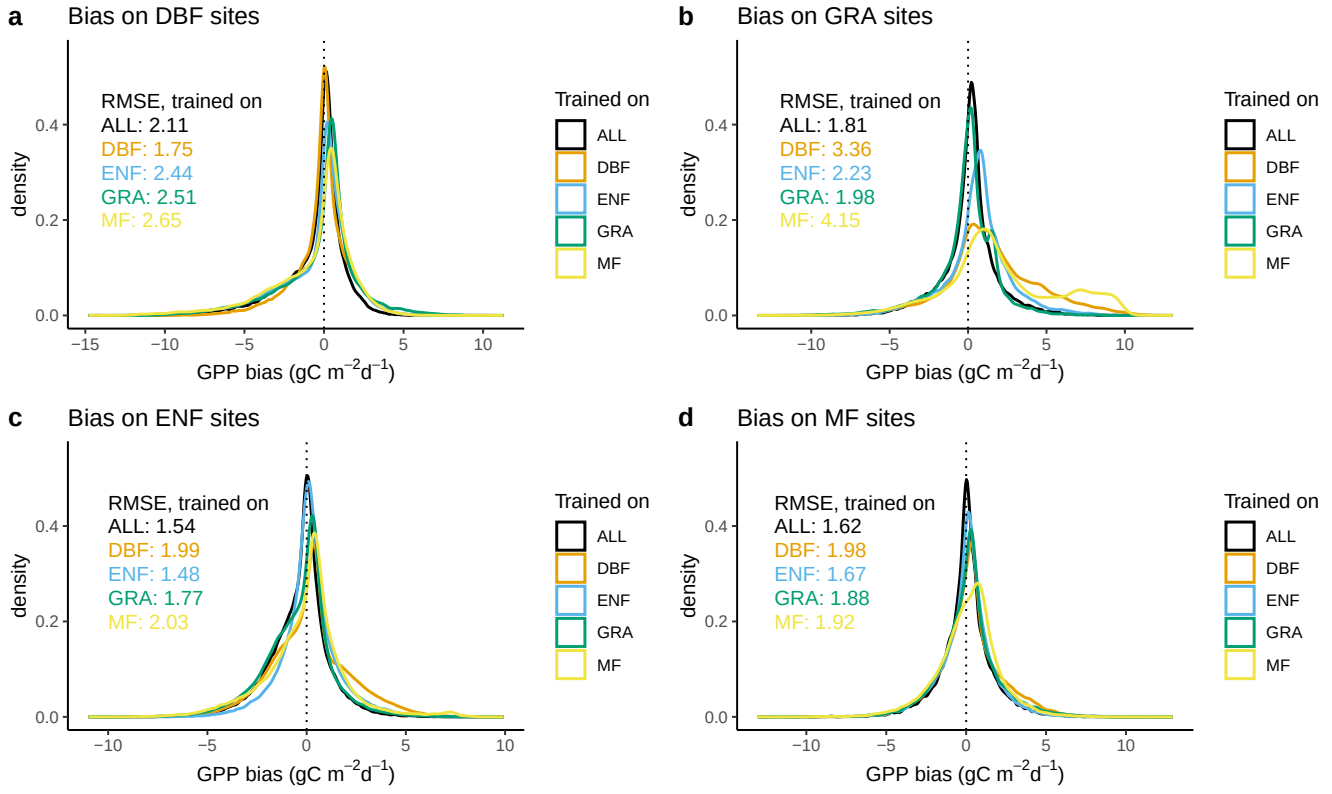

Figure 6. LGOCV for vegetation types. Shown are the distributions of the bias of daily GPP predictions for sites belonging to a given vegetation type, performed with a model trained on data from individual, other vegetation types, or from all vegetation types combined ('ALL'). 'DBF' is deciduous broadleaved forest, 'MF' is mixed forest, 'GRA' is grassland, 'ENF' is evergreen needle-leaved forest.

3.5 Generalisability across continents

The LGOCV with continents shows that model predictions for US sites have a smaller RMSE and average bias when the model is trained on only data from US sites (RMSE $= 1.42$ gC m^{-2} d^{-1}), than when the model is trained on only non-US sites' data (RMSE $= 1.84$ gC m^{-2} d^{-1}, Fig. 7). Note that the leave-site-out CV scheme was applied also for training and predicting within the same continent. Similarly, predictions for European sites are better for the model trained on only European sites (RMSE $= 1.74$ gC m^{-2} d^{-1}), compared to the model trained on data from non-European sites (RMSE $= 2.23$ gC m^{-2} d^{-1}). However, predictions of the model trained on data from sites of all continents ('ALL', RMSE $= 1.74$ gC m^{-2} d^{-1}) are equally good as within-Europe training and predictions. The distribution of the bias exhibits distinct patterns for the different models. For

https://doi.org/10.5194/egusphere-2023-1826
Preprint. Discussion started: 5 September 2023

example, for predictions on US sites with the model trained on non-US sites, the distribution is skewed to the right, indicating that GPP is often overestimated by that model.

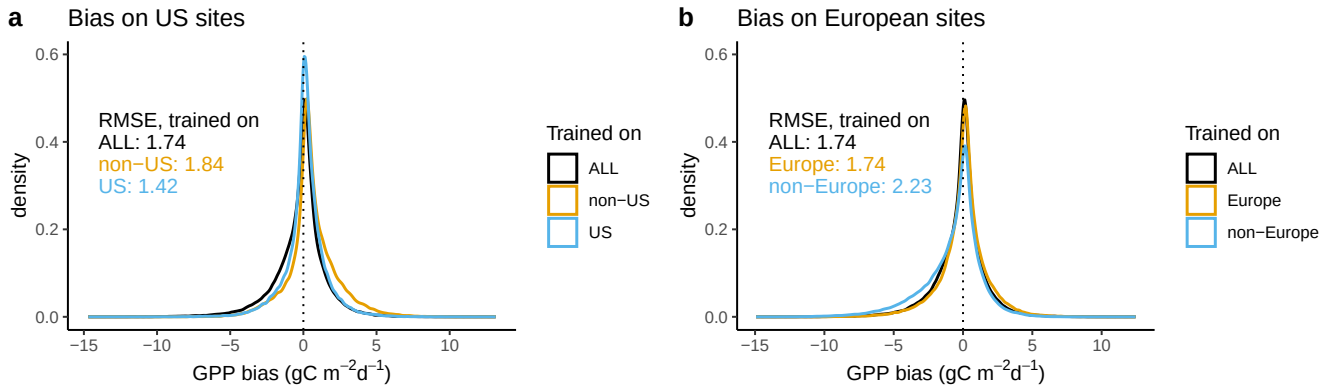

Figure 7. LGOCV for continents. Shown are the distributions of the bias of daily GPP predictions for sites belonging to a given continent, performed with a model trained on data from outside this continent, or from data of all continents ('ALL'). 'DBF' is a deciduous broadleaved forest, 'MF' is a mixed forest, 'GRA' is grassland, and 'ENF' is an evergreen needle-leaved forest. Distribution of the bias of predictions on sites of the "left-out continent", where the model was trained on all sites of one continent and tested on all sites from the other continent. 'EU' stands for Europe, and 'US' for the United States.

4 Discussion

4.1 Recurrent neural networks are suitable for modeling GPP

LSTMs are suitable for modelling GPP, better than a DNN, and achieve better predictions for the sites investigated here than a theory-based model. This is shown by the almost unanimous improvement of out-of-sample predictions for all sites by the LSTM model compared to the DNN and compared to the P-model (Fig. 3).

The LSTM's power in modelling GPP reflects its ability to learn temporal structure in the data and memory effects in the data-generating system (the ecosystem). Examples of known processes that introduce memory effects in environment-ecosystem flux relationships include the acclimation of plant physiology, in particular photosynthesis, to seasonally varying temperatures and light (Mäkelä et al., 2004; Luo and Keenan, 2020b; Jiang et al., 2020; Kumarathunge et al., 2019b), or root-zone moisture dynamics (Seneviratne et al., 2010; Teuling et al., 2006). The two processes differ in that they affect either the plants' abiotic environment (soil water potentials across the rooting profile) or the process responsible for the vegetation-atmosphere exchange itself (acclimation of photosynthesis). The former could, in principle, be continuously monitored and resulting information could be used for GPP modelling. However, practical and conceptual obstacles exist. Conceptual challenges include unknown effective rooting depth and spatial heterogeneity of plant water availability in the footprint of the flux tower. Recurrent neural networks offer a way to implicitly learn the actual, memory-dependent environment experienced by plants - even

https://doi.org/10.5194/egusphere-2023-1826
Preprint. Discussion started: 5 September 2023

in the absence of direct measurements of the same. The state of acclimation of plant physiology is probably more challenging to monitor. However, remotely sensed spectral canopy reflectance data reflects abiotic effects on plant physiology (Magney et al., 2019; D'Odorico et al., 2021) and may yield useful information for modelling respective effects on ecosystem fluxes. Such information may be particularly useful for modelling fluxes with non-recurrent neural networks and other algorithms that assume data to be IID.

We found a relatively poor performance of all models in simulating annual anomalies. Notably, also the recurrent neural network (the LSTM) performed weakly in capturing long-term dependencies, e.g., legacy effects of vegetation stress. This is possibly due to the limited length of training data from individual sites, or unexplained variations stemming from measurement uncertainty (e.g., sensor replacements) or stand development for which no information is captured by the predictors used here.

The LSTM also outperformed the theory-based model. This reflects the power of machine learning models to effectively exploit information in the data for an (often narrowly defined) prediction task, here GPP as a single target variable. This effectiveness stems from the machine learning models' flexibility in representing functional dependencies and their large number of parameters. In contrast, the theory-based model used here relies on *a priori* specified functional dependencies, a simplified representation of some processes (e.g., the radiative transfer in the canopy or plant hydraulics are not explicitly simulated in the model applied here), and relies on a very small number of parameters (here three), limiting the model to exploit the information contained in the data. The parameter-richness of deep neural networks comes with a risk of overfitting to the training data and poor generalisability to new data - here, new sites, geographic locations, environmental conditions, or vegetation types that are not represented in the training data. However, the LSOCV strategy applied here suggests that potential overfitting did not compromise the deep learning models' ability to accurately predict GPP. Yet, the environmental space in which the LSOCV was performed is limited and doesn't cover several major biomes and climate zones (Fig. 1). Furthermore, superior predictions of machine learning models come at the cost of limited model interpretability and the narrow scope of predictions of a single quantity (here GPP) for which training data is (and has to be) abundant. In contrast, the theory-based model applied here yields corollary predictions for connected ecosystem and plant states, traits, and rates (e.g., photosynthetic capacities (Smith et al., 2019) or leaf respiration rates (Wang et al., 2020)), that may be relevant in other modelling contexts (e.g., as a component of a land surface or Earth system model) but have different and often very limited direct observational constraints and calibration target data.

It should be noted that all the LSTM and DNN models were trained on data from years when atmospheric CO_2 was around 380-400 ppm, without actually considering ambient CO_2 as a predictor. Since CO_2 is known to affect photosynthesis, these models' applicability is thus limited to conditions with similar atmospheric CO_2 concentrations and CO_2-driven multi-annual GPP trends cannot be captured.

4.2 Challenges in modelling GPP at some, but not all dry sites

The various out-of-sample evaluation strategies applied here yield a nuanced picture of model generalisability and its limitations. The leave-site-out cross-validation indicated that GPP can be modelled confidently in seasonally radiation and temperature-limited and relatively moist temperate and boreal forests, where the LSTM achieved an R^2 in the LSOCV test of >0.9 at several

https://doi.org/10.5194/egusphere-2023-1826
Preprint. Discussion started: 5 September 2023

sites (Tab. 1). The dominant radiation-control of GPP implies a very regular seasonal cycle, determined largely by the site's latitude and the Earth's orbit, which can be confidently modelled.

Although the model skill found for moist temperate and boreal sites indicates good performance overall, distinct patterns in the model bias persist also at these sites. For example, a positive GPP bias in the early spring is found for many, but not all sites (Fig. 4). This reflects similar findings made in the evaluation of the P-model in simulating the seasonal GPP course in boreal and moist temperate sites (Stocker et al., 2020) and may be related to delayed effects of freezing temperatures and a slow recovery of photosynthetic activity after the temperature-limited dormant season (Mäkelä et al., 2008). Notably, the LSTM model doesn't "learn" such seasonal GPP dynamics in spite of its potential capacity to model temporal dependencies. This is possibly due to the fact that such dynamics are not operating at all sites and insufficient information (e.g., the identity of dominant species) is contained in the predictors for the model to "learn" where the slow spring-time recovery of photosynthesis is effective.

The LSOCV indicated poor model performance in predicting GPP at several, but not all (seasonally) dry sites. This suggests that the main source of out-of-sample prediction error is related to the uncertain effects of water limitation across sites. Although water and energy inputs (precipitation and net radiation), atmospheric water demand (vapour pressure deficit), and vegetation greenness are known from observations and used as model predictors here, there appears to be insufficient information for modelling the actual *exposure* of the vegetation to water stress. The very variable LSOCV model skill across relatively dry sites (ranging from an R^2 of 0.50 for AU-DaS to 0.86 for AU-ASM, Fig. 3) indicates that the relationship between ecosystem water and radiation inputs and water stress exposure is highly variable and insufficient information is provided through the predictors used for modelling here. Variable water stress exposure is likely linked to unknown rooting structure, soil water holding capacity and depth, and the presence (or absence) of extensive plant-accessible belowground water stores (lateral subsurface flow, groundwater or a perched water table) that enable (or prevent) sustained vegetation activity during long dry periods (Stocker et al., 2023; Fan et al., 2017; Trugman et al., 2021; Callahan et al., 2022).

4.3 Limitations to model generalisability

The basic rationale for spatial up-scaling of temporal or static ecological data is that training samples, although potentially geographically clustered, cover a wide enough environmental space to model relationships between the environment and the ecological target variable across a larger spatial domain. Since environmental variables (climate, soil, elevation, etc.) can be obtained from datasets with global coverage, the ecological target variable can be mapped globally, based on relationships learned from data obtained from a limited number of sites (e.g., Hengl et al. (2014); Ma et al. (2021); Dechant et al. (2023)). An additional premise of this approach (often considered but sometimes violated) is that the relationship between the ecological target variable and environmental predictors has no explicit dependency on the geographical location and that longitude and latitude are not included as predictors in the model. Thus, spatial autocorrelations in the predicted quantity can only arise due to (true) spatial autocorrelation in the environment, but not due to an (artefactual) autocorrelation resulting from geographical proximity of training and test sites. Here, we did not use geographical coordinates as model predictors and we investigated spatial generalisability by separating training and test sites by continents. This corresponds to a spatial cross-validation strategy,

https://doi.org/10.5194/egusphere-2023-1826
Preprint. Discussion started: 5 September 2023

which has been advocated (Roberts et al., 2017) (but also questioned (Sweet et al., 2023)) for similar spatial generalisation tasks.

We found that the far-range spatial model generalisability (across continents) was indeed hampered (Fig. 7). However, this finding may reflect limitations to the representativity of environmental conditions and biotic features, not geographical space, when limiting model training data to sites from a single continent. Yet, limited representativity of biotic features could also stem from distinct floral compositions across continents which reflects evolutionary history and constraints to species migration across geographical space. This would be a case in which geographical space has an explicit influence on environment-GPP relationships, but this interpretation remains speculative.

A further limitation to model generalisability was found with respect to vegetation types. Unless a certain vegetation type is represented in the training data, model predictions for the same deteriorate (Fig. 6). Due to limited data availability from savannah and shrub vegetation, we could only assess this form of generalisability for (evergreen, deciduous, and mixed) forests and grasslands. Also, moist tropical forests, characterised by particularly high foliage areas and tall tree statures, were not represented here. We also trained an LSTM model that had access to both temporally varying and time-invariant predictors. Time invariant predictors included vegetation type identity. Surprisingly, the LSTM variant exhibited no improvement in its predictions over the LSTM that was forced with only temporally varying predictors (not shown). This indicates that time series, most likely that of fAPAR, encode sufficient information for the model to discriminate between vegetation types, and/or that dependencies of fluxes on the environment (given fAPAR information) are similar across vegetation types - possibly a reflection of the common basic processes and controls that drive (mostly C_3) photosynthesis across the sites and species represented in our dataset.

Nevertheless, although the environmental space of the Earth's land surface is (and will always be) sparsely sampled by ecosystem flux measurement networks (Papale et al., 2015; Villarreal and Vargas, 2021), our results of the LSOCV suggests that there is sufficient data for models to learn from available observations and predict to new sites that were not "seen" during model training, and thus to "fill in" the un-sampled environmental domain - at least under conditions where water limitation is not a major driver of fluxes. However, the large domain of the environmental space that lies beyond what is covered by the site network (Fig. 1), in combination with the limits to model generalisability identified here, suggests considerable limitations to global upscaling on the basis of the site network used here.

4.4 Comparison to previous publications

The clearly superior model performance of the LSTM versus the non-recurrent DNN for simulating GPP found here contrasts with the findings reported by Besnard et al. (2019) who simulated net ecosystem exchange (NEE) with an LSTM. These authors found no clear improvement over predictions from non-recurrent models and interpreted their finding as an indication of either negligible signals of long-term legacy effects of stressors, limited temporal resolution of the data (monthly), or limited data quality (frequent cloud contamination and unreliable information for capturing disturbances and spatial context in the remote sensing data) (Besnard et al., 2019).

https://doi.org/10.5194/egusphere-2023-1826
Preprint. Discussion started: 5 September 2023

Contrasting model performances for predicting NEE versus GPP with a similar model trained on similar data may also be linked to smaller seasonal and spatial signals in NEE, compared to GPP time series. Smaller signals may be expected in view of compensating effects by ecosystem respiration (Reco, NEE = Reco - GPP), which exhibits similar frequencies, magnitudes, and timings of variations as GPP.

Further model improvements may be achieved by the use of more extensive training data that has recently become available, covering additional sites and years, the inclusion of additional remote sensing-based predictors that reflect environmental stressors on plant physiology (e.g., multi-spectral reflectance, sun-induced fluorescence, land surface temperature), and/or the consideration of other time-invariant data that encode information, useful for modelling water stress exposure or vegetation type and canopy structure. The relatively narrow selection of training (and testing) sites considered here is a limitation that may easily be relieved in future studies.

5 Conclusions

Taken together, we demonstrated that an LSTM - a recurrent deep neural network - is suitable for predicting ecosystem GPP, given observations of a set of meteorological variables and remotely sensed estimates of the fraction of radiation absorbed by the vegetation canopy. The LSTM performs superior compared to a non-recurrent DNN and a relatively simple, parameter-sparse theoretical model. We have also demonstrated that the LSTM performs well at new sites, not "seen" during model training - suggesting the model's ability to spatially upscale GPP estimates across larger spatial domains on the basis of spatially mapped meteorological and remotely sensed covariates.

However, cross-validation by vegetation types and across continents indicated limits to far-range up-scalability (spatial generalisability) across a global domain with widely varying vegetation types, floral compositions, and climate conditions that are not or only very sparsely sampled by a subset of the eddy covariance measurement network used here.

Code and data availability. Code for the LSTM and DNN models is published on Zenodo (DOI:10.5281/zenodo.8210649). Development code of the same repository is on GitHub at https://github.com/geco-bern/mlflx2.

Author contributions. P.D.B., A.M., and Z.S. implemented the models, training, and testing, ran the experiments, analysed the results, and contributed to writing the manuscript. B.D.S. designed the research, wrote the manuscript, and produced visualisations.

Competing interests. The authors declare no competing interests.

https://doi.org/10.5194/egusphere-2023-1826
Preprint. Discussion started: 5 September 2023

Acknowledgements. We thank Fanny Yang for feedback on the research design. B.D.S was funded by the Swiss National Science Foundation grant no. PCEFP2_181115. This work is a contribution to the LEMONTREE (Land Ecosystem Models based On New Theory, obseRvations and ExperimEnts) project, funded through the generosity of Eric and Wendy Schmidt by recommendation of the Schmidt Futures program (BDS).

https://doi.org/10.5194/egusphere-2023-1826
Preprint. Discussion started: 5 September 2023

References

Ahlström, A., Raupach, M. R., Schurgers, G., Smith, B., Arneth, A., Jung, M., Reichstein, M., Canadell, J. G., Friedlingstein, P., Jain, A. K., Kato, E., Poulter, B., Sitch, S., Stocker, B. D., Viovy, N., Wang, Y. P., Wiltshire, A., Zaehle, S., and Zeng, N.: The dominant role of semi-arid ecosystems in the trend and variability of the land CO2 sink, Science, 348, 895–899, https://doi.org/10.1126/science.aaa1668, 2015.

Ammann, C., Spirig, C., Leifeld, J., and Neftel, A.: Assessment of the nitrogen and carbon budget of two managed temperate grassland fields, Agriculture, Ecosystems & Environment, 133, 150–162, https://doi.org/10.1016/j.agee.2009.05.006, 2009.

Anthoni, P. M., Knohl, A., Rebmann, C., Freibauer, A., Mund, M., Ziegler, W., Kolle, O., and Schulze, E.-D.: Forest and agricultural land-use-dependent CO2 exchange in Thuringia, Germany, Global Change Biology, 10, 2005–2019, https://doi.org/10.1111/j.1365-2486.2004.00863.x, 2004.

Aubinet, M., Chermanne, B., Vandenhaute, M., Longdoz, B., Yernaux, M., and Laitat, E.: Long term carbon dioxide exchange above a mixed forest in the Belgian Ardennes, Agricultural and Forest Meteorology, 108, 293–315, https://doi.org/10.1016/s0168-1923(01)00244-1, 2001.

Baldocchi, D., Chen, Q., Chen, X., Ma, S., Miller, G., Ryu, Y., Xiao, J., Wenk, R., and Battles, J.: The Dynamics of Energy, Water, and Carbon Fluxes in a Blue Oak (Quercus douglasii) Savanna in California, in: Ecosystem Function in Savannas, pp. 135–151, CRC Press, https://doi.org/10.1201/b10275-10, 2010.

Baldocchi, D. D.: Must we incorporate soil moisture information when applying light use efficiency models with satellite remote sensing information?, New Phytol., 218, 1293–1294, 2018.

Baldocchi, D. D.: How eddy covariance flux measurements have contributed to our understanding of Global Change Biology, Global Change Biology, 26, 242–260, https://doi.org/https://doi.org/10.1111/gcb.14807, 2020.

Barber, J. and Andersson, B.: Too much of a good thing: light can be bad for photosynthesis, Trends in Biochemical Sciences, 17, 61–66, https://doi.org/https://doi.org/10.1016/0968-0004(92)90503-2, 1992.

Bastos, A., Ciais, P., Friedlingstein, P., Sitch, S., Pongratz, J., Fan, L., Wigneron, J. P., Weber, U., Reichstein, M., Fu, Z., Anthoni, P., Arneth, A., Haverd, V., Jain, A. K., Joetzjer, E., Knauer, J., Lienert, S., Loughran, T., McGuire, P. C., Tian, H., Viovy, N., and Zaehle, S.: Direct and seasonal legacy effects of the 2018 heat wave and drought on European ecosystem productivity, Science Advances, 6, eaba2724, https://doi.org/10.1126/sciadv.aba2724, 2020.

Beck, H. E., Zimmermann, N. E., McVicar, T. R., Vergopolan, N., Berg, A., and Wood, E. F.: Present and future Köppen-Geiger climate classification maps at 1-km resolution, Scientific Data, 5, 180 214, https://doi.org/10.1038/sdata.2018.214, 2018.

Beer, C., Reichstein, M., Tomelleri, E., Ciais, P., Jung, M., Carvalhais, N., Rödenbeck, C., Arain, M. A., Baldocchi, D., Bonan, G. B., Bondeau, A., Cescatti, A., Lasslop, G., Lindroth, A., Lomas, M., Luyssaert, S., Margolis, H., Oleson, K. W., Roupsard, O., Veenendaal, E., Viovy, N., Williams, C., Woodward, F. I., and Papale, D.: Terrestrial gross carbon dioxide uptake: global distribution and covariation with climate, Science, 329, 834–838, 2010.

Berbigier, P., Bonnefond, J.-M., and Mellmann, P.: CO2 and water vapour fluxes for 2 years above Euroflux forest site, Agricultural and Forest Meteorology, 108, 183–197, https://doi.org/10.1016/s0168-1923(01)00240-4, 2001.

Beringer, J., Hutley, L. B., Tapper, N. J., and Cernusak, L. A.: Savanna fires and their impact on net ecosystem productivity in North Australia, Global Change Biology, 13, 990–1004, https://doi.org/10.1111/j.1365-2486.2007.01334.x, 2007.

https://doi.org/10.5194/egusphere-2023-1826
Preprint. Discussion started: 5 September 2023

Beringer, J., Hutley, L. B., Hacker, J. M., Neininger, B., and U, K. T. P.: Patterns and processes of carbon, water and energy cycles across northern Australian landscapes: From point to region, Agricultural and Forest Meteorology, 151, 1409–1416, https://doi.org/10.1016/j.agrformet.2011.05.003, 2011a.

Beringer, J., Hutley, L. B., Hacker, J. M., Neininger, B., and U, K. T. P.: Patterns and processes of carbon, water and energy cycles across northern Australian landscapes: From point to region, Agricultural and Forest Meteorology, 151, 1409–1416, https://doi.org/10.1016/j.agrformet.2011.05.003, 2011b.

Beringer, J., Livesley, S. J., Randle, J., and Hutley, L. B.: Carbon dioxide fluxes dominate the greenhouse gas exchanges of a seasonal wetland in the wet–dry tropics of northern Australia, Agricultural and Forest Meteorology, 182-183, 239–247, https://doi.org/10.1016/j.agrformet.2013.06.008, 2013.

Besnard, S., Carvalhais, N., Arain, M. A., Black, A., Brede, B., Buchmann, N., Chen, J., Clevers, J. G. P. W., Dutrieux, L. P., Gans, F., Herold, M., Jung, M., Kosugi, Y., Knohl, A., Law, B. E., Paul-Limoges, E., Lohila, A., Merbold, L., Roupsard, O., Valentini, R., Wolf, S., Zhang, X., and Reichstein, M.: Memory effects of climate and vegetation affecting net ecosystem CO2 fluxes in global forests, PLOS ONE, 14, e0211 510, https://doi.org/10.1371/journal.pone.0211510, 2019.

Callahan, R. P., Riebe, C. S., Sklar, L. S., Pasquet, S., Ferrier, K. L., Hahm, W. J., Taylor, N. J., Grana, D., Flinchum, B. A., Hayes, J. L., and Holbrook, W. S.: Forest vulnerability to drought controlled by bedrock composition, Nature Geoscience, 15, 714–719, https://doi.org/10.1038/s41561-022-01012-2, 2022.

Carrara, A., Janssens, I. A., Yuste, J. C., and Ceulemans, R.: Seasonal changes in photosynthesis, respiration and NEE of a mixed temperate forest, Agricultural and Forest Meteorology, 126, 15–31, https://doi.org/10.1016/j.agrformet.2004.05.002, 2004.

Chiesi, M., Maselli, F., Bindi, M., Fibbi, L., Cherubini, P., Arlotta, E., Tirone, G., Matteucci, G., and Seufert, G.: Modelling carbon budget of Mediterranean forests using ground and remote sensing measurements, Agricultural and Forest Meteorology, 135, 22–34, https://doi.org/10.1016/j.agrformet.2005.09.011, 2005.

Chu, H., Luo, X., Ouyang, Z., Chan, W. S., Dengel, S., Biraud, S. C., Torn, M. S., Metzger, S., Kumar, J., Arain, M. A., Arkebauer, T. J., Baldocchi, D., Bernacchi, C., Billesbach, D., Black, T. A., Blanken, P. D., Bohrer, G., Bracho, R., Brown, S., Brunsell, N. A., Chen, J., Chen, X., Clark, K., Desai, A. R., Duman, T., Durden, D., Fares, S., Forbrich, I., Gamon, J. A., Gough, C. M., Griffis, T., Helbig, M., Hollinger, D., Humphreys, E., Ikawa, H., Iwata, H., Ju, Y., Knowles, J. F., Knox, S. H., Kobayashi, H., Kolb, T., Law, B., Lee, X., Litvak, M., Liu, H., Munger, J. W., Noormets, A., Novick, K., Oberbauer, S. F., Oechel, W., Oikawa, P., Papuga, S. A., Pendall, E., Prajapati, P., Prueger, J., Quinton, W. L., Richardson, A. D., Russell, E. S., Scott, R. L., Starr, G., Staebler, R., Stoy, P. C., Stuart-Haëntjens, E., Sonnentag, O., Sullivan, R. C., Suyker, A., Ueyama, M., Vargas, R., Wood, J. D., and Zona, D.: Representativeness of Eddy-Covariance flux footprints for areas surrounding AmeriFlux sites, Agricultural and Forest Meteorology, 301-302, 108 350, https://doi.org/10.1016/j.agrformet.2021.108350, 2021.

Ciais, P., Reichstein, M., Viovy, N., Granier, A., Ogée, J., Allard, V., Aubinet, M., Buchmann, N., Bernhofer, C., Carrara, A., Chevallier, F., De Noblet, N., Friend, A. D., Friedlingstein, P., Grünwald, T., Heinesch, B., Keronen, P., Knohl, A., Krinner, G., Loustau, D., Manca, G., Matteucci, G., Miglietta, F., Ourcival, J. M., Papale, D., Pilegaard, K., Rambal, S., Seufert, G., Soussana, J. F., Sanz, M. J., Schulze, E. D., Vesala, T., and Valentini, R.: Europe-wide reduction in primary productivity caused by the heat and drought in 2003, Nature, 437, 529–533, https://doi.org/10.1038/nature03972, 2005.

Cleverly, J., Boulain, N., Villalobos-Vega, R., Grant, N., Faux, R., Wood, C., Cook, P. G., Yu, Q., Leigh, A., and Eamus, D.: Dynamics of component carbon fluxes in a semi-arid Acacia woodland, central Australia, Journal of Geophysical Research: Biogeosciences, 118, 1168–1185, https://doi.org/10.1002/jgrg.20101, 2013.

https://doi.org/10.5194/egusphere-2023-1826
Preprint. Discussion started: 5 September 2023

D., S. and L., M.: Application of LSTM Neural Networks in Language Modelling, Text, Speech, and Dialogue, 8082, https://doi.org/10.1007/978-3-642-40585-3_14, 2013.

Davis, T. W., Prentice, I. C., Stocker, B. D., Thomas, R. T., Whitley, R. J., Wang, H., Evans, B. J., Gallego-Sala, A. V., Sykes, M. T., and Cramer, W.: Simple process-led algorithms for simulating habitats (SPLASH v.1.0): robust indices of radiation, evapotranspiration and plant-available moisture, Geoscientific Model Development, 10, 689–708, https://doi.org/10.5194/gmd-10-689-2017, 2017.

Dechant, B., Kattge, J., Pavlick, R., Schneider, F., Sabatini, F., Moreno-Martinez, A., Butler, E., Bodegom, P. v., Vallicrosa, H., Kattenborn, T., Boonman, C., Madani, N., Wright, I., Dong, N., Feilhauer, H., Penuelas, J., Sardans, J., Aguirre-Gutierrez, J., Reich, P., Leitao, P., Cavender-Bares, J., Myers-Smith, I. H., Duran, S., Croft, H., Prentice, I. C., Huth, A., Rebel, K., Zaehle, S., Simova, I., Diaz, S., Reichstein, M., Schiller, C., Bruehlheide, H., Mahecha, M., Wirth, C., Malhi, Y., and Townsend, P.: Intercomparison of global foliar trait maps reveals fundamental differences and limitations of upscaling approaches, https://eartharxiv.org/repository/view/5266/, publisher: EarthArXiv, 2023.

Delpierre, N., Berveiller, D., Granda, E., and Dufrêne, E.: Wood phenology, not carbon input, controls the interannual variability of wood growth in a temperate oak forest, New Phytologist, 210, 459–470, https://doi.org/10.1111/nph.13771, 2015.

Desai, A. R., Xu, K., Tian, H., Weishampel, P., Thom, J., Baumann, D., Andrews, A. E., Cook, B. D., King, J. Y., and Kolka, R.: Landscape-level terrestrial methane flux observed from a very tall tower, Agricultural and Forest Meteorology, 201, 61–75, https://doi.org/10.1016/j.agrformet.2014.10.017, 2015.

D'Odorico, P., Schönbeck, L., Vitali, V., Meusburger, K., Schaub, M., Ginzler, C., Zweifel, R., Velasco, V. M. E., Gisler, J., Gessler, A., and Ensminger, I.: Drone-based physiological index reveals long-term acclimation and drought stress responses in trees, Plant, Cell & Environment, 44, 3552–3570, https://doi.org/10.1111/pce.14177, 2021.

Dragoni, D., Schmid, H. P., Wayson, C. A., Potter, H., Grimmond, C. S. B., and Randolph, J. C.: Evidence of increased net ecosystem productivity associated with a longer vegetated season in a deciduous forest in south-central Indiana, USA, Global Change Biology, 17, 886–897, https://doi.org/10.1111/j.1365-2486.2010.02281.x, 2011.

Dušek, J., Čížková, H., Stellner, S., Czerný, R., and Květ, J.: Fluctuating water table affects gross ecosystem production and gross radiation use efficiency in a sedge-grass marsh, Hydrobiologia, 692, 57–66, https://doi.org/10.1007/s10750-012-0998-z, 2012.

Elsworth, S. and Güttel, S.: Time Series Forecasting Using LSTM Networks: A Symbolic Approach, arXiv:2003.05672, https://arxiv.org/abs/2003.05672, 2020.

Etzold, S., Ruehr, N. K., Zweifel, R., Dobbertin, M., Zingg, A., Pluess, P., Häsler, R., Eugster, W., and Buchmann, N.: The Carbon Balance of Two Contrasting Mountain Forest Ecosystems in Switzerland: Similar Annual Trends, but Seasonal Differences, Ecosystems, 14, 1289–1309, https://doi.org/10.1007/s10021-011-9481-3, 2011.

Fan, Y., Miguez-Macho, G., Jobbágy, E. G., Jackson, R. B., and Otero-Casal, C.: Hydrologic regulation of plant rooting depth, Proceedings of the National Academy of Sciences, 114, 10 572–10 577, https://doi.org/10.1073/pnas.1712381114, 2017.

Fares, S., Savi, F., Muller, J., Matteucci, G., and Paoletti, E.: Simultaneous measurements of above and below canopy ozone fluxes help partitioning ozone deposition between its various sinks in a Mediterranean Oak Forest, Agricultural and Forest Meteorology, 198-199, 181–191, https://doi.org/10.1016/j.agrformet.2014.08.014, 2014.

Ferréa, C., Zenone, T., Comolli, R., and Seufert, G.: Estimating heterotrophic and autotrophic soil respiration in a semi-natural forest of Lombardy, Italy, Pedobiologia, 55, 285–294, https://doi.org/10.1016/j.pedobi.2012.05.001, 2012.

https://doi.org/10.5194/egusphere-2023-1826
Preprint. Discussion started: 5 September 2023

Frank, J. M., Massman, W. J., Ewers, B. E., Huckaby, L. S., and Negrón, J. F.: Ecosystem CO2/H2O fluxes are explained by hydraulically limited gas exchange during tree mortality from spruce bark beetles, Journal of Geophysical Research: Biogeosciences, 119, 1195–1215, https://doi.org/10.1002/2013jg002597, 2014.

Galvagno, M., Wohlfahrt, G., Cremonese, E., Rossini, M., Colombo, R., Filippa, G., Julitta, T., Manca, G., Siniscalco, C., di Cella, U. M., and Migliavacca, M.: Phenology and carbon dioxide source/sink strength of a subalpine grassland in response to an exceptionally short snow season, Environmental Research Letters, 8, 025 008, https://doi.org/10.1088/1748-9326/8/2/025008, 2013.

Gamon, J. A., Huemmrich, K. F., Wong, C. Y. S., Ensminger, I., Garrity, S., Hollinger, D. Y., Noormets, A., and Peñuelas, J.: A remotely sensed pigment index reveals photosynthetic phenology in evergreen conifers, Proceedings of the National Academy of Sciences, 113, 13 087–13 092, 2016.

Gough, C. M., Hardiman, B. S., Nave, L. E., Bohrer, G., Maurer, K. D., Vogel, C. S., Nadelhoffer, K. J., and Curtis, P. S.: Sustained carbon uptake and storage following moderate disturbance in a Great Lakes forest, Ecological Applications, 23, 1202–1215, https://doi.org/10.1890/12-1554.1, 2013a.

Gough, C. M., Hardiman, B. S., Nave, L. E., Bohrer, G., Maurer, K. D., Vogel, C. S., Nadelhoffer, K. J., and Curtis, P. S.: Sustained carbon uptake and storage following moderate disturbance in a Great Lakes forest, Ecological Applications, 23, 1202–1215, https://doi.org/10.1890/12-1554.1, 2013b.

Grünwald, T. and Bernhofer, C.: A decade of carbon, water and energy flux measurements of an old spruce forest at the Anchor Station Tharandt, Tellus B, 59, 387–396, https://doi.org/10.1111/j.1600-0889.2007.00259.x, 2007.

Hengl, T., de Jesus, J. M., MacMillan, R. A., Batjes, N. H., Heuvelink, G. B. M., Ribeiro, E., Samuel-Rosa, A., Kempen, B., Leenaars, J. G. B., Walsh, M. G., and Gonzalez, M. R.: SoilGrids1km — Global Soil Information Based on Automated Mapping, PLOS ONE, 9, 1–17, https://doi.org/10.1371/journal.pone.0105992, 2014.

Hinko-Najera, N., Isaac, P., Beringer, J., van Gorsel, E., Ewenz, C., McHugh, I., Exbrayat, J.-F., Livesley, S. J., and Arndt, S. K.: Net ecosystem carbon exchange of a dry temperate eucalypt forest, Biogeosciences, 14, 3781–3800, https://doi.org/10.5194/bg-14-3781-2017, 2017.

Hochreiter, S. and Schmidhuber, J.: Long short-term memory, Neural computation, 9, 1735–1780, 1997.

Hoshika, Y., Fares, S., Savi, F., Gruening, C., Goded, I., De Marco, A., Sicard, P., and Paoletti, E.: Stomatal conductance models for ozone risk assessment at canopy level in two Mediterranean evergreen forests, Agricultural and Forest Meteorology, 234-235, 212–221, https://doi.org/10.1016/j.agrformet.2017.01.005, 2017.

Hutley, L. B., Beringer, J., Isaac, P. R., Hacker, J. M., and Cernusak, L. A.: A sub-continental scale living laboratory: Spatial patterns of savanna vegetation over a rainfall gradient in northern Australia, Agricultural and Forest Meteorology, 151, 1417–1428, https://doi.org/10.1016/j.agrformet.2011.03.002, 2011.

Imer, D., Merbold, L., Eugster, W., and Buchmann, N.: Temporal and spatial variations of soil CO_2, CH_4 and N_2O fluxes at three differently managed grasslands, Biogeosciences, 10, 5931–5945, https://doi.org/10.5194/bg-10-5931-2013, 2013.

Irvine, J., Law, B. E., Martin, J. G., and Vickers, D.: Interannual variation in soil CO2 efflux and the response of root respiration to climate and canopy gas exchange in mature ponderosa pine, Global Change Biology, 14, 2848–2859, https://doi.org/10.1111/j.1365-2486.2008.01682.x, 2008.

Jacobs, C. M. J., Jacobs, A. F. G., Bosveld, F. C., Hendriks, D. M. D., Hensen, A., Kroon, P. S., Moors, E. J., Nol, L., Schrier-Uijl, A., and Veenendaal, E. M.: Variability of annual CO_2 exchange from Dutch grasslands, Biogeosciences, 4, 803–816, https://doi.org/10.5194/bg-4-803-2007, 2007.

https://doi.org/10.5194/egusphere-2023-1826
Preprint. Discussion started: 5 September 2023

Jiang, C., Ryu, Y., Wang, H., and Keenan, T. F.: An optimality-based model explains seasonal variation in C3 plant photosynthetic capacity, Global Change Biology, 26, 6493–6510, https://doi.org/https://doi.org/10.1111/gcb.15276, 2020.

Jung, M., Reichstein, M., Ciais, P., Seneviratne, S. I., Sheffield, J., Goulden, M. L., Bonan, G., Cescatti, A., Chen, J., de Jeu, R., Dolman, A. J., Eugster, W., Gerten, D., Gianelle, D., Gobron, N., Heinke, J., Kimball, J., Law, B. E., Montagnani, L., Mu, Q., Mueller, B., Oleson, K., Papale, D., Richardson, A. D., Roupsard, O., Running, S., Tomelleri, E., Viovy, N., Weber, U., Williams, C., Wood, E., Zaehle, S., and Zhang, K.: Recent decline in the global land evapotranspiration trend due to limited moisture supply, Nature, 467, 951–954, 2010.

Jung, M., Reichstein, M., Margolis, H. A., Cescatti, A., Richardson, A. D., Arain, M. A., Arneth, A., Bernhofer, C., Bonal, D., Chen, J., Gianelle, D., Gobron, N., Kiely, G., Kutsch, W., Lasslop, G., Law, B. E., Lindroth, A., Merbold, L., Montagnani, L., Moors, E. J., Papale, D., Sottocornola, M., Vaccari, F., and Williams, C.: Global patterns of land-atmosphere fluxes of carbon dioxide, latent heat, and sensible heat derived from eddy covariance, satellite, and meteorological observations, Journal of Geophysical Research: Biogeosciences, 116, 2011.

Jung, M., Schwalm, C., Migliavacca, M., Walther, S., Camps-Valls, G., Koirala, S., Anthoni, P., Besnard, S., Bodesheim, P., Carvalhais, N., Chevallier, F., Gans, F., Goll, D. S., Haverd, V., Köhler, P., Ichii, K., Jain, A. K., Liu, J., Lombardozzi, D., Nabel, J. E. M., Nelson, J. A., O'Sullivan, M., Pallandt, M., Papale, D., Peters, W., Pongratz, J., Rödenbeck, C., Sitch, S., Tramontana, G., Walker, A., Weber, U., and Reichstein, M.: Scaling carbon fluxes from eddy covariance sites to globe: synthesis and evaluation of the FLUXCOM approach, 2020.

Knohl, A., Schulze, E.-D., Kolle, O., and Buchmann, N.: Large carbon uptake by an unmanaged 250-year-old deciduous forest in Central Germany, Agricultural and Forest Meteorology, 118, 151–167, https://doi.org/10.1016/s0168-1923(03)00115-1, 2003.

Kumarathunge, D. P., Medlyn, B. E., Drake, J. E., Tjoelker, M. G., Aspinwall, M. J., Battaglia, M., Cano, F. J., Carter, K. R., Cavaleri, M. A., Cernusak, L. A., Chambers, J. Q., Crous, K. Y., De Kauwe, M. G., Dillaway, D. N., Dreyer, E., Ellsworth, D. S., Ghannoum, O., Han, Q., Hikosaka, K., Jensen, A. M., Kelly, J. W. G., Kruger, E. L., Mercado, L. M., Onoda, Y., Reich, P. B., Rogers, A., Slot, M., Smith, N. G., Tarvainen, L., Tissue, D. T., Togashi, H. F., Tribuzy, E. S., Uddling, J., Vårhammar, A., Wallin, G., Warren, J. M., and Way, D. A.: Acclimation and adaptation components of the temperature dependence of plant photosynthesis at the global scale, New Phytol., 222, 768–784, 2019a.

Kumarathunge, D. P., Medlyn, B. E., Drake, J. E., Tjoelker, M. G., Aspinwall, M. J., Battaglia, M., Cano, F. J., Carter, K. R., Cavaleri, M. A., Cernusak, L. A., Chambers, J. Q., Crous, K. Y., De Kauwe, M. G., Dillaway, D. N., Dreyer, E., Ellsworth, D. S., Ghannoum, O., Han, Q., Hikosaka, K., Jensen, A. M., Kelly, J. W. G., Kruger, E. L., Mercado, L. M., Onoda, Y., Reich, P. B., Rogers, A., Slot, M., Smith, N. G., Tarvainen, L., Tissue, D. T., Togashi, H. F., Tribuzy, E. S., Uddling, J., Vårhammar, A., Wallin, G., Warren, J. M., and Way, D. A.: Acclimation and adaptation components of the temperature dependence of plant photosynthesis at the global scale, New Phytol., 222, 768–784, 2019b.

Kurbatova, J., Li, C., Varlagin, A., Xiao, X., and Vygodskaya, N.: Modeling carbon dynamics in two adjacent spruce forests with different soil conditions in Russia, Biogeosciences, 5, 969–980, https://doi.org/10.5194/bg-5-969-2008, 2008.

Luo, X. and Keenan, T. F.: Global evidence for the acclimation of ecosystem photosynthesis to light, Nat Ecol Evol, 4, 1351–1357, 2020a.

Luo, X. and Keenan, T. F.: Global evidence for the acclimation of ecosystem photosynthesis to light, Nat Ecol Evol, 4, 1351–1357, 2020b.

Ma, H., Mo, L., Crowther, T. W., Maynard, D. S., van den Hoogen, J., Stocker, B. D., Terrer, C., and Zohner, C. M.: The global distribution and environmental drivers of aboveground versus belowground plant biomass, Nature Ecology & Evolution, 5, 1110–1122, https://doi.org/10.1038/s41559-021-01485-1, 2021.

Ma, S., Baldocchi, D. D., Xu, L., and Hehn, T.: Inter-annual variability in carbon dioxide exchange of an oak/grass savanna and open grassland in California, Agricultural and Forest Meteorology, 147, 157–171, https://doi.org/10.1016/j.agrformet.2007.07.008, 2007.

https://doi.org/10.5194/egusphere-2023-1826
Preprint. Discussion started: 5 September 2023

Magney, T. S., Bowling, D. R., Logan, B. A., Grossmann, K., Stutz, J., Blanken, P. D., Burns, S. P., Cheng, R., Garcia, M. A., Khler, P., Lopez, S., Parazoo, N. C., Raczka, B., Schimel, D., and Frankenberg, C.: Mechanistic evidence for tracking the seasonality of photosynthesis with solar-induced fluorescence, Proceedings of the National Academy of Sciences, 116, 11 640–11 645, https://doi.org/10.1073/pnas.1900278116, 2019.

Maire, V., Martre, P., Kattge, J., Gastal, F., Esser, G., Fontaine, S., and Soussana, J.-F.: The Coordination of Leaf Photosynthesis Links C and N Fluxes in C3 Plant Species, PLOS ONE, 7, 1–15, https://doi.org/10.1371/journal.pone.0038345, 2012.

Marcolla, B., Pitacco, A., and Cescatti, A.: Canopy Architecture and Turbulence Structure in a Coniferous Forest, Boundary-Layer Meteorology, 108, 39–59, https://doi.org/10.1023/a:1023027709805, 2003.

Marcolla, B., Cescatti, A., Manca, G., Zorer, R., Cavagna, M., Fiora, A., Gianelle, D., Rodeghiero, M., Sottocornola, M., and Zampedri, R.: Climatic controls and ecosystem responses drive the inter-annual variability of the net ecosystem exchange of an alpine meadow, Agricultural and Forest Meteorology, 151, 1233–1243, https://doi.org/10.1016/j.agrformet.2011.04.015, 2011.

Matsumoto, K., Ohta, T., Nakai, T., Kuwada, T., Daikoku, K., Iida, S., Yabuki, H., Kononov, A. V., van der Molen, M. K., Kodama, Y., Maximov, T. C., Dolman, A. J., and Hattori, S.: Energy consumption and evapotranspiration at several boreal and temperate forests in the Far East, Agricultural and Forest Meteorology, 148, 1978–1989, https://doi.org/10.1016/j.agrformet.2008.09.008, 2008.

McDowell, N. G., Sapes, G., Pivovaroff, A., Adams, H. D., Allen, C. D., Anderegg, W. R. L., Arend, M., Breshears, D. D., Brodribb, T., Choat, B., Cochard, H., De Cáceres, M., De Kauwe, M. G., Grossiord, C., Hammond, W. M., Hartmann, H., Hoch, G., Kahmen, A., Klein, T., Mackay, D. S., Mantova, M., Martínez-Vilalta, J., Medlyn, B. E., Mencuccini, M., Nardini, A., Oliveira, R. S., Sala, A., Tissue, D. T., Torres-Ruiz, J. M., Trowbridge, A. M., Trugman, A. T., Wiley, E., and Xu, C.: Mechanisms of woody-plant mortality under rising drought, CO2 and vapour pressure deficit, Nature Reviews Earth & Environment, 3, 294–308, https://doi.org/10.1038/s43017-022-00272-1, 2022.

McHugh, I. D., Beringer, J., Cunningham, S. C., Baker, P. J., Cavagnaro, T. R., Nally, R. M., and Thompson, R. M.: Interactions between nocturnal turbulent flux, storage and advection at an "ideal" eucalypt woodland site, Biogeosciences, 14, 3027–3050, https://doi.org/10.5194/bg-14-3027-2017, 2017.

Meyer, H. and Pebesma, E.: Machine learning-based global maps of ecological variables and the challenge of assessing them, Nature Communications, 13, 2208, https://doi.org/10.1038/s41467-022-29838-9, 2022.

Migliavacca, M., Meroni, M., Busetto, L., Colombo, R., Zenone, T., Matteucci, G., Manca, G., and Seufert, G.: Modeling Gross Primary Production of Agro-Forestry Ecosystems by Assimilation of Satellite-Derived Information in a Process-Based Model, Sensors, 9, 922–942, https://doi.org/10.3390/s90200922, 2009.

Monteith, J. L.: Solar Radiation and Productivity in Tropical Ecosystems, J. Appl. Ecol., 9, 747–766, 1972.

Moors, E.: Water Use of Forests in The Netherlands, Ph.D. thesis, Vrije Universiteit Amsterdam, 2012.

Myneni, R., Knyazikhin, Y., and Park, T.: MCD15A3H MODIS/Terra+Aqua Leaf Area Index/FPAR 4-day L4 Global 500m SIN Grid V006, https://doi.org/10.5067/MODIS/MCD15A3H.006, https://doi.org/10.5067/MODIS/MCD15A3H.006, 2015.

Mäkelä, A., Hari, P., Berninger, F., Hänninen, H., and Nikinmaa, E.: Acclimation of photosynthetic capacity in Scots pine to the annual cycle of temperature, Tree Physiol., 24, 369–376, 2004.

Mäkelä, A., Pulkkinen, M., Kolari, P., Lagergren, F., Berbigier, P., Lindroth, A., Loustau, D., Nikinmaa, E., Vesala, T., and Hari, P.: Developing an empirical model of stand GPP with the LUE approach: analysis of eddy covariance data at five contrasting conifer sites in Europe, Global Change Biology, 14, 92–108, https://doi.org/10.1111/j.1365-2486.2007.01463.x, _eprint: https://onlinelibrary.wiley.com/doi/pdf/10.1111/j.1365-2486.2007.01463.x, 2008.

https://doi.org/10.5194/egusphere-2023-1826
Preprint. Discussion started: 5 September 2023

Novick, K. A., Ficklin, D. L., Stoy, P. C., Williams, C. A., Bohrer, G., Christopher Oishi, A., Papuga, S. A., Blanken, P. D., Noormets, A., Sulman, B. N., Scott, R. L., Wang, L., and Phillips, R. P.: The increasing importance of atmospheric demand for ecosystem water and carbon fluxes, 2016.

Papale, D., Migliavacca, M., Cremonese, E., Cescatti, A., Alberti, G., Balzarolo, M., Marchesini, L. B., Canfora, E., Casa, R., Duce, P., Facini, O., Galvagno, M., Genesio, L., Gianelle, D., Magliulo, V., Matteucci, G., Montagnani, L., Petrella, F., Pitacco, A., Seufert, G., Spano, D., Stefani, P., Vaccari, F. P., and Valentini, R.: Carbon, Water and Energy Fluxes of Terrestrial Ecosystems in Italy, in: The Greenhouse Gas Balance of Italy, pp. 11–45, Springer Berlin Heidelberg, https://doi.org/10.1007/978-3-642-32424-6_2, 2014.

Papale, D., Black, T. A., Carvalhais, N., Cescatti, A., Chen, J., Jung, M., Kiely, G., Lasslop, G., Mahecha, M. D., Margolis, H., Merbold, L., Montagnani, L., Moors, E., Olesen, J. E., Reichstein, M., Tramontana, G., Gorsel, E., Wohlfahrt, G., and Ráduly, B.: Effect of spatial sampling from European flux towers for estimating carbon and water fluxes with artificial neural networks, Journal of Geophysical Research: Biogeosciences, 120, 1941–1957, https://doi.org/10.1002/2015JG002997, 2015.

Pastorello, G., Trotta, C., Canfora, E., Chu, H., Christianson, D., Cheah, Y.-W., Poindexter, C., Chen, J., Elbashandy, A., Humphrey, M., Isaac, P., Polidori, D., Reichstein, M., Ribeca, A., van Ingen, C., Vuichard, N., Zhang, L., Amiro, B., Ammann, C., Arain, M. A., Ardö, J., Arkebauer, T., Arndt, S. K., Arriga, N., Aubinet, M., Aurela, M., Baldocchi, D., Barr, A., Beamesderfer, E., Marchesini, L. B., Bergeron, O., Beringer, J., Bernhofer, C., Berveiller, D., Billesbach, D., Black, T. A., Blanken, P. D., Bohrer, G., Boike, J., Bolstad, P. V., Bonal, D., Bonnefond, J.-M., Bowling, D. R., Bracho, R., Brodeur, J., Brümmer, C., Buchmann, N., Burban, B., Burns, S. P., Buysse, P., Cale, P., Cavagna, M., Cellier, P., Chen, S., Chini, I., Christensen, T. R., Cleverly, J., Collalti, A., Consalvo, C., Cook, B. D., Cook, D., Coursolle, C., Cremonese, E., Curtis, P. S., D'Andrea, E., da Rocha, H., Dai, X., Davis, K. J., Cinti, B. D., Grandcourt, A. d., Ligne, A. D., De Oliveira, R. C., Delpierre, N., Desai, A. R., Di Bella, C. M., Tommasi, P. d., Dolman, H., Domingo, F., Dong, G., Dore, S., Duce, P., Dufrêne, E., Dunn, A., Dušek, J., Eamus, D., Eichelmann, U., ElKhidir, H. A. M., Eugster, W., Ewenz, C. M., Ewers, B., Famulari, D., Fares, S., Feigenwinter, I., Feitz, A., Fensholt, R., Filippa, G., Fischer, M., Frank, J., Galvagno, M., Gharun, M., Gianelle, D., Gielen, B., Gioli, B., Gitelson, A., Goded, I., Goeckede, M., Goldstein, A. H., Gough, C. M., Goulden, M. L., Graf, A., Griebel, A., Gruening, C., Grünwald, T., Hammerle, A., Han, S., Han, X., Hansen, B. U., Hanson, C., Hatakka, J., He, Y., Hehn, M., Heinesch, B., Hinko-Najera, N., Hörtnagl, L., Hutley, L., Ibrom, A., Ikawa, H., Jackowicz-Korczynski, M., Janouš, D., Jans, W., Jassal, R., Jiang, S., Kato, T., Khomik, M., Klatt, J., Knohl, A., Knox, S., Kobayashi, H., Koerber, G., Kolle, O., Kosugi, Y., Kotani, A., Kowalski, A., Kruijt, B., Kurbatova, J., Kutsch, W. L., Kwon, H., Launiainen, S., Laurila, T., Law, B., Leuning, R., Li, Y., Liddell, M., Limousin, J.-M., Lion, M., Liska, A. J., Lohila, A., López-Ballesteros, A., López-Blanco, E., Loubet, B., Loustau, D., Lucas-Moffat, A., Lüers, J., Ma, S., Macfarlane, C., Magliulo, V., Maier, R., Mammarella, I., Manca, G., Marcolla, B., Margolis, H. A., Marras, S., Massman, W., Mastepanov, M., Matamala, R., Matthes, J. H., Mazzenga, F., McCaughey, H., McHugh, I., McMillan, A. M. S., Merbold, L., Meyer, W., Meyers, T., Miller, S. D., Minerbi, S., Moderow, U., Monson, R. K., Montagnani, L., Moore, C. E., Moors, E., Moreaux, V., Moureaux, C., Munger, J. W., Nakai, T., Neirynck, J., Nesic, Z., Nicolini, G., Noormets, A., Northwood, M., Nosetto, M., Nouvellon, Y., Novick, K., Oechel, W., Olesen, J. E., Ourcival, J.-M., Papuga, S. A., Parmentier, F.-J., Paul-Limoges, E., Pavelka, M., Peichl, M., Pendall, E., Phillips, R. P., Pilegaard, K., Pirk, N., Posse, G., Powell, T., Prasse, H., Prober, S. M., Rambal, S., Rannik, Ü., Raz-Yaseef, N., Rebmann, C., Reed, D., Dios, V. R. d., Restrepo-Coupe, N., Reverter, B. R., Roland, M., Sabbatini, S., Sachs, T., Saleska, S. R., Sánchez-Cañete, E. P., Sanchez-Mejia, Z. M., Schmid, H. P., Schmidt, M., Schneider, K., Schrader, F., Schroder, I., Scott, R. L., Sedlák, P., Serrano-Ortíz, P., Shao, C., Shi, P., Shironya, I., Siebicke, L., Šigut, L., Silberstein, R., Sirca, C., Spano, D., Steinbrecher, R., Stevens, R. M., Sturtevant, C., Suyker, A., Tagesson, T., Takanashi, S., Tang, Y., Tapper, N., Thom, J., Tomassucci, M., Tuovinen, J.-P., Urbanski, S., Valentini, R., van der Molen, M., van Gorsel, E., van Huissteden, K., Varlagin, A., Verfaillie, J., Vesala, T., Vincke, C., Vitale, D., Vygodskaya, N., Walker, J. P., Walter-Shea, E., Wang, H., Weber, R.,

https://doi.org/10.5194/egusphere-2023-1826
Preprint. Discussion started: 5 September 2023

Westermann, S., Wille, C., Wofsy, S., Wohlfahrt, G., Wolf, S., Woodgate, W., Li, Y., Zampedri, R., Zhang, J., Zhou, G., Zona, D., Agarwal, D., Biraud, S., Torn, M., and Papale, D.: The FLUXNET2015 dataset and the ONEFlux processing pipeline for eddy covariance data, Sci Data, 7, 225, 2020a.

Pastorello, G., Trotta, C., Canfora, E., Chu, H., Christianson, D., Cheah, Y.-W., Poindexter, C., Chen, J., Elbashandy, A., Humphrey, M., et al.: The FLUXNET2015 dataset and the ONEFlux processing pipeline for eddy covariance data, Scientific data, 7, 1–27, 2020b.

Paszke, A., Gross, S., Massa, F., Lerer, A., Bradbury, J., Chanan, G., Killeen, T., Lin, Z., Gimelshein, N., Antiga, L., Desmaison, A., Kopf, A., Yang, E., DeVito, Z., Raison, M., Tejani, A., Chilamkurthy, S., Steiner, B., Fang, L., Bai, J., and Chintala, S.: PyTorch: An Imperative Style, High-Performance Deep Learning Library, in: Advances in Neural Information Processing Systems 32, edited by Wallach, H., Larochelle, H., Beygelzimer, A., d'Alché-Buc, F., Fox, E., and Garnett, R., pp. 8024–8035, Curran Associates, Inc., http://papers.neurips.cc/paper/9015-pytorch-an-imperative-style-high-performance-deep-learning-library.pdf, 2019.

Peng, S., Ciais, P., Chevallier, F., Peylin, P., Cadule, P., Sitch, S., Piao, S., Ahlström, A., Huntingford, C., Levy, P., Li, X., Liu, Y., Lomas, M., Poulter, B., Viovy, N., Wang, T., Wang, X., Zaehle, S., Zeng, N., Zhao, F., and Zhao, H.: Benchmarking the seasonal cycle of CO2fluxes simulated by terrestrial ecosystem models, 2015.

Pilegaard, K., Ibrom, A., Courtney, M. S., Hummelshøj, P., and Jensen, N. O.: Increasing net CO2 uptake by a Danish beech forest during the period from 1996 to 2009, Agricultural and Forest Meteorology, 151, 934–946, https://doi.org/10.1016/j.agrformet.2011.02.013, 2011.

Ploton, P., Mortier, F., Réjou-Méchain, M., Barbier, N., Picard, N., Rossi, V., Dormann, C., Cornu, G., Viennois, G., Bayol, N., Lyapustin, A., Gourlet-Fleury, S., and Pélissier, R.: Spatial validation reveals poor predictive performance of large-scale ecological mapping models, Nature Communications, 11, 4540, https://doi.org/10.1038/s41467-020-18321-y, 2020.

Post, H., Franssen, H. J. H., Graf, A., Schmidt, M., and Vereecken, H.: Uncertainty analysis of eddy covariance CO_2 flux measurements for different EC tower distances using an extended two-tower approach, Biogeosciences, 12, 1205–1221, https://doi.org/10.5194/bg-12-1205-2015, 2015.

Prentice, I. C., Dong, N., Gleason, S. M., Maire, V., and Wright, I. J.: Balancing the costs of carbon gain and water transport: testing a new theoretical framework for plant functional ecology, Ecology Letters, 17, 82–91, https://doi.org/10.1111/ele.12211, 2014.

Prescher, A.-K., Grünwald, T., and Bernhofer, C.: Land use regulates carbon budgets in eastern Germany: From NEE to NBP, Agricultural and Forest Meteorology, 150, 1016–1025, https://doi.org/10.1016/j.agrformet.2010.03.008, 2010a.

Prescher, A.-K., Grünwald, T., and Bernhofer, C.: Land use regulates carbon budgets in eastern Germany: From NEE to NBP, Agricultural and Forest Meteorology, 150, 1016–1025, https://doi.org/10.1016/j.agrformet.2010.03.008, 2010b.

Priestley, C. H. B. and Taylor, R. J.: On the assessment of surface heat flux and evaporation using large-scale parameters, Monthly Weather Review, 100, 81–92, 1972.

Rambal, S., Joffre, R., Ourcival, J. M., Cavender-Bares, J., and Rocheteau, A.: The growth respiration component in eddy CO2 flux from a Quercus ilex mediterranean forest, Global Change Biology, 10, 1460–1469, https://doi.org/10.1111/j.1365-2486.2004.00819.x, 2004.

Reichstein, M., Falge, E., Baldocchi, D., Papale, D., Aubinet, M., Berbigier, P., Bernhofer, C., Buchmann, N., Gilmanov, T., Granier, A., Grünwald, T., Havránková, K., Ilvesniemi, H., Janous, D., Knohl, A., Laurila, T., Lohila, A., Loustau, D., Matteucci, G., Meyers, T., Miglietta, F., Ourcival, J.-M., Pumpanen, J., Rambal, S., Rotenberg, E., Sanz, M., Tenhunen, J., Seufert, G., Vaccari, F., Vesala, T., Yakir, D., and Valentini, R.: On the separation of net ecosystem exchange into assimilation and ecosystem respiration: review and improved algorithm, Global Change Biology, 11, 1424–1439, https://doi.org/https://doi.org/10.1111/j.1365-2486.2005.001002.x, 2005.

https://doi.org/10.5194/egusphere-2023-1826
Preprint. Discussion started: 5 September 2023

Roberts, D. R., Bahn, V., Ciuti, S., Boyce, M. S., Elith, J., Guillera-Arroita, G., Hauenstein, S., Lahoz-Monfort, J. J., Schröder, B., Thuiller, W., Warton, D. I., Wintle, B. A., Hartig, F., and Dormann, C. F.: Cross-validation strategies for data with temporal, spatial, hierarchical, or phylogenetic structure, Ecography, 40, 913–929, https://doi.org/10.1111/ecog.02881, 2017.

Ryu, Y., Berry, J. A., and Baldocchi, D. D.: What is global photosynthesis? History, uncertainties and opportunities, Remote Sens. Environ., 223, 95–114, 2019.

Scott, R. L., Jenerette, G. D., Potts, D. L., and Huxman, T. E.: Effects of seasonal drought on net carbon dioxide exchange from a woody-plant-encroached semiarid grassland, Journal of Geophysical Research: Biogeosciences, 114, https://doi.org/10.1029/2008JG000900, 2009.

Scott, R. L., Biederman, J. A., Hamerlynck, E. P., and Barron-Gafford, G. A.: The carbon balance pivot point of southwestern U.S. semiarid ecosystems: Insights from the 21st century drought, Journal of Geophysical Research: Biogeosciences, 120, 2612–2624, https://doi.org/10.1002/2015jg003181, 2015.

Seneviratne, S. I., Corti, T., Davin, E. L., Hirschi, M., Jaeger, E. B., Lehner, I., Orlowsky, B., and Teuling, A. J.: Investigating soil moisture–climate interactions in a changing climate: A review, Earth-Science Reviews, 99, 125–161, https://doi.org/10.1016/j.earscirev.2010.02.004, 2010.

Smith, N. G., Keenan, T. F., Colin Prentice, I., Wang, H., Wright, I. J., Niinemets, , Crous, K. Y., Domingues, T. F., Guerrieri, R., Yoko Ishida, F., Kattge, J., Kruger, E. L., Maire, V., Rogers, A., Serbin, S. P., Tarvainen, L., Togashi, H. F., Townsend, P. A., Wang, M., Weerasinghe, L. K., and Zhou, S.-X.: Global photosynthetic capacity is optimized to the environment, Ecology Letters, 22, 506–517, https://doi.org/10.1111/ele.13210, 2019.

Stefan, V. and Levin, S.: plotbiomes: Plot Whittaker biomes with ggplot2, r package version 0.0.0.9001, 2023.

Stocker, B. and Hufkens, K.: ingestr v1.3: R package for environmental data ingest, https://doi.org/10.5281/zenodo.5531240, 2021.

Stocker, B. D., Wang, H., Smith, N. G., Harrison, S. P., Keenan, T. F., Sandoval, D., Davis, T., and Prentice, I. C.: P-model v1.0: an optimality-based light use efficiency model for simulating ecosystem gross primary production, Geosci. Model Dev., 13, 1545–1581, 2015.

Stocker, B. D., Zscheischler, J., Keenan, T. F., Colin Prentice, I., Peñuelas, J., and Seneviratne, S. I.: Quantifying soil moisture impacts on light use efficiency across biomes, 2018a.

Stocker, B. D., Zscheischler, J., Keenan, T. F., Prentice, I. C., Peñuelas, J., and Seneviratne, S. I.: Quantifying soil moisture impacts on light use efficiency across biomes, New Phytologist, 218, 1430–1449, 2018b.

Stocker, B. D., Wang, H., Smith, N. G., Harrison, S. P., Keenan, T. F., Sandoval, D., Davis, T., and Prentice, I. C.: P-model v1.0: an optimality-based light use efficiency model for simulating ecosystem gross primary production, Geoscientific Model Development, 13, 1545–1581, https://doi.org/10.5194/gmd-13-1545-2020, 2020.

Stocker, B. D., Tumber-Dávila, S. J., Konings, A. G., Anderson, M. C., Hain, C., and Jackson, R. B.: Global patterns of water storage in the rooting zones of vegetation, Nature Geoscience, pp. 1–7, https://doi.org/10.1038/s41561-023-01125-2, publisher: Nature Publishing Group, 2023.

Sun, Z., Wang, X., Yamamoto, H., Tani, H., Zhong, G., Yin, S., and Guo, E.: Spatial pattern of GPP variations in terrestrial ecosystems and its drivers: Climatic factors, CO2 concentration and land-cover change, 1982–2015, 2018.

Suni, T., Rinne, J., Reissel, A., Altimir, N., Keronen, P., Rannik, Ü., Maso, M., Kulmala, M., and Vesala, T.: Long-term measurements of surface fluxes above a Scots pine forest in Hyytiälä, southern Finland, Boreal Environ. Res., 4, 287–301, 2003.

Sweet, L.-b., Müller, C., Anand, M., and Zscheischler, J.: Cross-validation strategy impacts the performance and interpretation of machine learning models, Artificial Intelligence for the Earth Systems, -1, 1–35, https://doi.org/10.1175/AIES-D-23-0026.1, publisher: American Meteorological Society Section: Artificial Intelligence for the Earth Systems, 2023.

https://doi.org/10.5194/egusphere-2023-1826
Preprint. Discussion started: 5 September 2023

Teuling, A. J., Seneviratne, S. I., Williams, C., and Troch, P. A.: Observed timescales of evapotranspiration response to soil moisture, Geophysical Research Letters, 33, 2006.

Thum, T., Aalto, T., Laurila, T., Aurela, M., Kolari, P., and Hari, P.: Parametrization of two photosynthesis models at the canopy scale in a northern boreal Scots pine forest, Tellus B, 59, https://doi.org/10.3402/tellusb.v59i5.17066, 2007.

Tramontana, G., Jung, M., Schwalm, C. R., Ichii, K., Camps-Valls, G., Ráduly, B., Reichstein, M., Altaf Arain, M., Cescatti, A., Kiely, G., Merbold, L., Serrano-Ortiz, P., Sickert, S., Wolf, S., and Papale, D.: Predicting carbon dioxide and energy fluxes across global FLUXNET sites with regression algorithms, 2016.

Trugman, A. T., Anderegg, L. D., Anderegg, W. R., Das, A. J., and Stephenson, N. L.: Why is Tree Drought Mortality so Hard to Predict?, Trends in Ecology & Evolution, 36, 520–532, https://doi.org/10.1016/j.tree.2021.02.001, 2021.

Tuck, S. L., Phillips, H. R., Hintzen, R. E., Scharlemann, J. P., Purvis, A., and Hudson, L. N.: MODISTools – downloading and processing MODIS remotely sensed data in R, Ecology and Evolution, 4, 4658–4668, https://doi.org/10.1002/ece3.1273, 2014.

Tuzet, A., Perrier, A., and Leuning, R.: A coupled model of stomatal conductance, photosynthesis and transpiration, 2003.

Urbanski, S., Barford, C., Wofsy, S., Kucharik, C., Pyle, E., Budney, J., McKain, K., Fitzjarrald, D., Czikowsky, M., and Munger, J. W.: Factors controlling CO2 exchange on timescales from hourly to decadal at Harvard Forest, Journal of Geophysical Research: Biogeosciences, 112, https://doi.org/10.1029/2006JG000293, 2007.

Villarreal, S. and Vargas, R.: Representativeness of FLUXNET Sites Across Latin America, Journal of Geophysical Research: Biogeosciences, 126, e2020JG006 090, https://doi.org/10.1029/2020JG006090, _eprint: https://onlinelibrary.wiley.com/doi/pdf/10.1029/2020JG006090, 2021.

Wang, H., Prentice, I. C., and Davis, T. W.: Biophsyical constraints on gross primary production by the terrestrial biosphere, Biogeosciences, 11, 5987–6001, https://doi.org/10.5194/bg-11-5987-2014, 2014.

Wang, H., Prentice, I. C., Keenan, T. F., Davis, T. W., Wright, I. J., Cornwell, W. K., Evans, B. J., and Peng, C.: Towards a universal model for carbon dioxide uptake by plants, Nat Plants, 3, 734–741, 2017.

Wang, H., Atkin, O. K., Keenan, T. F., Smith, N. G., Wright, I. J., Bloomfield, K. J., Kattge, J., Reich, P. B., and Prentice, I. C.: Acclimation of leaf respiration consistent with optimal photosynthetic capacity, Global Change Biology, 26, 2573–2583, https://doi.org/10.1111/gcb.14980, _eprint: https://onlinelibrary.wiley.com/doi/pdf/10.1111/gcb.14980, 2020.

Wen, X. F., Wang, H. M., Wang, J. L., Yu, G. R., and Sun, X. M.: Ecosystem carbon exchanges of a subtropical evergreen coniferous plantation subjected to seasonal drought, 2003-2007, Biogeosciences, 7, 357–369, https://doi.org/10.5194/bg-7-357-2010, 2010.

Whittaker, R. H.: Classification of Natural Communities, Botanical Review, 28, 1–239, https://www.jstor.org/stable/4353649, publisher: New York Botanical Garden Press, 1962.

Wiltshire, A. J., Rojas, M. C. D., Edwards, J. M., Gedney, N., Harper, A. B., Hartley, A. J., Hendry, M. A., Robertson, E., and Smout-Day, K.: JULES-GL7: the Global Land configuration of the Joint UK Land Environment Simulator version 7.0 and 7.2, 2020.

Xiao, J., Zhuang, Q., Law, B. E., Chen, J., Baldocchi, D. D., Cook, D. R., Oren, R., Richardson, A. D., Wharton, S., and Ma, S.: A continuous measure of gross primary production for the conterminous United States derived from MODIS and AmeriFlux data, 2010.

Yang, F., Ichii, K., White, M. A., Hashimoto, H., Michaelis, A. R., Votava, P., Zhu, A.-X., Huete, A., Running, S. W., and Nemani, R. R.: Developing a continental-scale measure of gross primary production by combining MODIS and AmeriFlux data through Support Vector Machine approach, 2007.

Yang Xiang, Gubian, S., Suomela, B., and Hoeng, J.: Generalized Simulated Annealing for Efficient Global Optimization: the GenSA Package for R., The R Journal Volume 5/1, June 2013, http://journal.r-project.org/, 2013.

https://doi.org/10.5194/egusphere-2023-1826
Preprint. Discussion started: 5 September 2023

760 Yu, X., Orth, R., Reichstein, M., Bahn, M., Klosterhalfen, A., Knohl, A., Koebsch, F., Migliavacca, M., Mund, M., Nelson, J. A., Stocker, B. D., Walther, S., and Bastos, A.: Contrasting drought legacy effects on gross primary productivity in a mixed versus pure beech forest, Biogeosciences Discussions, 2022, 1–27, https://doi.org/10.5194/bg-2022-99, 2022.

https://doi.org/10.5194/egusphere-2023-1826
Preprint. Discussion started: 5 September 2023

Site	Lon.	Lat.	Period	Veg.	Clim.	N	LSTM	DNN	P-model	Reference
AU-ASM	133.25	-22.28	2010-2013	ENF	BSh	1461	0.86	0.687	0.348	(Cleverly et al., 2013)
AU-DaP	131.32	-14.06	2007-2013	GRA	Aw	2557	0.81	0.798	0.415	(Beringer et al., 2011a)
AU-DaS	131.39	-14.16	2008-2014	SAV	Aw	2557	0.50	0.442	0.093	(Hutley et al., 2011)
AU-Fog	131.31	-12.55	2006-2008	WET	Aw	1095	0.73	0.012	0.162	(Beringer et al., 2013)
AU-How	131.15	-12.49	2001-2014	WSA	Aw	5113	0.62	0.506	0.039	(Beringer et al., 2007)
AU-Stp	133.35	-17.15	2008-2014	GRA	BSh	2557	0.78	0.632	0.431	(Beringer et al., 2011b)
AU-Whr	145.03	-36.67	2011-2014	EBF	Cfb	1461	0.50	0.382	0.556	(McHugh et al., 2017)
AU-Wom	144.09	-37.42	2010-2012	EBF	Cfb	1095	0.73	0.729	0.788	(Hinko-Najera et al., 2017)
BE-Bra	4.52	51.31	1996-2014	MF	Cfb	6940	0.81	0.760	0.733	(Carrara et al., 2004)
BE-Vie	6.00	50.31	1996-2014	MF	Cfb	6940	0.88	0.828	0.741	(Aubinet et al., 2001)
CH-Fru	8.54	47.12	2005-2014	GRA	Cfb	3652	0.79	0.779	0.715	(Imer et al., 2013)
CH-Lae	8.37	47.48	2004-2014	MF	Cfb	4018	0.71	0.691	0.647	(Etzold et al., 2011)
CH-Oe1	7.73	47.29	2002-2008	GRA	Cfb	2557	0.66	0.653	0.603	(Ammann et al., 2009)
CN-Qia	115.06	26.74	2003-2005	ENF	Cfa	1096	0.83	0.826	0.705	(Wen et al., 2010)
CZ-wet	14.77	49.02	2006-2014	WET	Cfb	3287	0.85	0.754	0.722	(Dušek et al., 2012)
DE-Geb	10.91	51.10	2001-2014	CRO	Cfb	5113	0.67	0.688	0.648	(Anthoni et al., 2004)
DE-Gri	13.51	50.95	2004-2014	GRA	Cfb	4018	0.76	0.784	0.719	(Prescher et al., 2010a)
DE-Hai	10.45	51.08	2000-2012	DBF	Cfb	4749	0.92	0.867	0.792	(Knohl et al., 2003)
DE-Kli	13.52	50.89	2004-2014	CRO	Cfb	4018	0.71	0.710	0.664	(Prescher et al., 2010b)
DE-Obe	13.72	50.78	2008-2014	ENF	Cfb	2557	0.90	0.859	0.781	NA
DE-RuR	6.30	50.62	2011-2014	GRA	Cfb	1461	0.80	0.774	0.662	(Post et al., 2015)
DE-Spw	14.03	51.89	2010-2014	WET	Cfb	1826	0.93	0.868	0.834	NA
DE-Tha	13.57	50.96	1996-2014	ENF	Cfb	6940	0.84	0.871	0.751	(Grünwald and Bernhofer, 2007)
DK-Sor	11.64	55.49	1996-2014	DBF	Cfb	6940	0.90	0.873	0.827	(Pilegaard et al., 2011)
FI-Hyy	24.30	61.85	1996-2014	ENF	Dfc	6940	0.93	0.887	0.805	(Suni et al., 2003)
FI-Sod	26.64	67.36	2001-2014	ENF	Dfc	5113	0.76	0.746	0.788	(Thum et al., 2007)
FR-Fon	2.78	48.48	2005-2014	DBF	Cfb	3652	0.91	0.830	0.749	(Delpierre et al., 2015)
FR-LBr	-0.77	44.72	1996-2008	ENF	Cfb	4749	0.73	0.715	0.657	(Berbigier et al., 2001)
FR-Pue	3.60	43.74	2000-2014	EBF	Csa	5479	0.55	0.496	0.391	(Rambal et al., 2004)
IT-Cp2	12.36	41.70	2012-2014	EBF	Csa	1096	0.55	0.535	0.477	(Fares et al., 2014)
IT-Isp	8.63	45.81	2013-2014	DBF	Cfb	730	0.90	0.851	0.835	(Ferréa et al., 2012)
IT-Lav	11.28	45.96	2003-2014	ENF	Cfb	4383	0.78	0.759	0.626	(Marcolla et al., 2003)
IT-MBo	11.05	46.01	2003-2013	GRA	Dfb	4018	0.86	0.849	0.790	(Marcolla et al., 2011)
IT-Noe	8.15	40.61	2004-2014	CSH	-	4018	0.53	0.315	0.262	(Papale et al., 2014)

Table 1. Sites used for evaluation and LSOCV results. Lon. is longitude, negative values indicate west longitude; Lat. is latitude, positive values indicate north latitude; Veg. is vegetation type: deciduous broadleaf forest (DBF); evergreen broadleaf forest (EBF); evergreen needleleaf forest (ENF); grassland (GRA); mixed deciduous and evergreen needleleaf forest (MF); savanna ecosystem (SAV); shrub ecosystem (SHR); wetland (WET). Columns 'LSTM', 'DNN', and 'P-model' contain the R^2 of predictions from the LSOCV.

https://doi.org/10.5194/egusphere-2023-1826
Preprint. Discussion started: 5 September 2023

Site	Lon.	Lat.	Period	Veg.	Clim.	N	LSTM	DNN	P-model	Reference
IT-PT1	9.06	45.20	2002-2004	DBF	Cfa	1095	0.92	0.917	0.856	(Migliavacca et al., 2009)
IT-SR2	10.29	43.73	2013-2014	ENF	Csa	730	0.84	0.825	0.814	(Hoshika et al., 2017)
IT-SRo	10.28	43.73	1999-2012	ENF	Csa	5114	0.62	0.620	0.565	(Chiesi et al., 2005)
IT-Tor	7.58	45.84	2008-2014	GRA	Dfc	2557	0.89	0.848	0.782	(Galvagno et al., 2013)
JP-SMF	137.08	35.26	2002-2006	MF	Cfa	1826	0.72	0.712	0.517	(Matsumoto et al., 2008)
NL-Hor	5.07	52.24	2004-2011	GRA	Cfb	2922	0.86	0.828	0.774	(Jacobs et al., 2007)
NL-Loo	5.74	52.17	1996-2013	ENF	Cfb	6574	0.87	0.821	0.762	(Moors, 2012)
RU-Fyo	32.92	56.46	1998-2014	ENF	Dfb	6209	0.86	0.833	0.741	(Kurbatova et al., 2008)
US-GLE	-106.24	41.37	2004-2014	ENF	Dfb	4018	0.83	0.791	0.789	(Frank et al., 2014)
US-Ha1	-72.17	42.54	1991-2012	DBF	Dfb	8036	0.84	0.819	0.763	(Urbanski et al., 2007)
US-Me2	-121.56	44.45	2002-2014	ENF	Csb	4748	0.73	0.721	0.703	(Irvine et al., 2008)
US-MMS	-86.41	39.32	1999-2014	DBF	Cfa	5844	0.92	0.867	0.761	(Dragoni et al., 2011)
US-PFa	-90.27	45.95	1995-2014	MF	Dfb	7305	0.86	0.777	0.759	(Desai et al., 2015)
US-SRG	-110.83	31.79	2008-2014	GRA	BSk	2557	0.79	0.724	0.534	(Scott et al., 2015)
US-SRM	-110.87	31.82	2004-2014	WSA	BSk	4018	0.82	0.718	0.507	(Scott et al., 2009)
US-Ton	-120.97	38.43	2001-2014	WSA	Csa	5113	0.67	0.634	0.488	(Baldocchi et al., 2010)
US-UMB	-84.71	45.56	2000-2014	DBF	Dfb	5479	0.93	0.906	0.865	(Gough et al., 2013a)
US-UMd	-84.70	45.56	2007-2014	DBF	Dfb	2922	0.94	0.891	0.824	(Gough et al., 2013b)
US-Var	-120.95	38.41	2000-2014	GRA	Csa	5479	0.65	0.616	0.304	(Ma et al., 2007)

Table 2. Sites used for evaluation and LSOCV results. Lon. is longitude, negative values indicate west longitude; Lat. is latitude, positive values indicate north latitude; Veg. is vegetation type: deciduous broadleaf forest (DBF); evergreen broadleaf forest (EBF); evergreen needleleaf forest (ENF); grassland (GRA); mixed deciduous and evergreen needleleaf forest (MF); savanna ecosystem (SAV); shrub ecosystem (SHR); wetland (WET). Columns 'LSTM', 'DNN', and 'P-model' contain the R^2 of predictions from the LSOCV.

Model	Daily*	Daily	Seasonal*	Seasonal	Spatial	Daily anom.*	Ann. anom.*
LSTM	0.78	0.82	0.91	0.92	0.88	0.37	0.34
DNN	0.73	0.77	0.86	0.88	0.78	0.32	0.34
P-model	0.64	0.64	0.78	0.74	0.35	0.29	0.36

Table 3. R^2 computed on predictions aggregated at different temporal scales. The '*' marks that the metrics are determined as a mean across site-level R^2, determined based on predictions from the LSOCV. All other metrics are derived from modelled and observed values pooled across all sites. 'Seasonal' refers to values aggregated by day-of-year and site. 'Spatial' refers to an evaluation of site-level means. 'Daily anom.' refers to the anomaly of daily values relative to a mean seasonal cycle. 'Ann. anom.' refers to the anomaly of annual means relative to the multi-year mean by site.